Accepted Manuscript

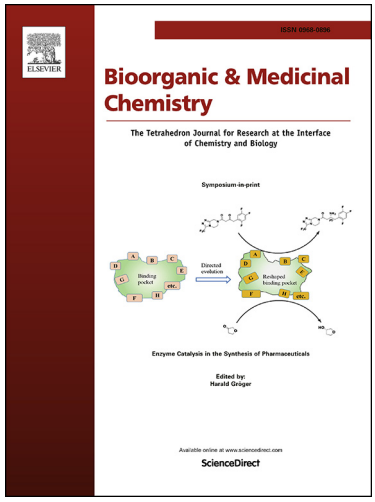

PPARγ-Sparing Thiazolidinediones as Insulin Sensitizers. Design, Synthesis and Selection of Compounds for Clinical Development

Steven P. Tanis, Jerry R. Colca, Timothy T. Parker, Gerald D.Artman III, Scott D. Larsen, William G. McDonald, Robert C. Gadwood, Rolf F. Kletzien, James B. Zeller, Pil H. Lee, Wade J. Adams

PII: S0968-0896(18)31564-5
DOI: https://doi.org/10.1016/j.bmc.2018.10.033
Reference: BMC 14592

To appear in: *Bioorganic & Medicinal Chemistry*

Received Date: 5 September 2018
Revised Date: 20 October 2018
Accepted Date: 27 October 2018

Please cite this article as: Tanis, S.P., Colca, J.R., Parker, T.T., D.Artman, G. III, Larsen, S.D., McDonald, W.G., Gadwood, R.C., Kletzien, R.F., Zeller, J.B., Lee, P.H., Adams, W.J., PPARγ-Sparing Thiazolidinediones as Insulin Sensitizers. Design, Synthesis and Selection of Compounds for Clinical Development, *Bioorganic & Medicinal Chemistry* (2018), doi: https://doi.org/10.1016/j.bmc.2018.10.033

PPARγ-Sparing Thiazolidinediones as Insulin Sensitizers. Design, Synthesis and Selection of Compounds for Clinical Development

Steven P. Tanis; [*a] Jerry R. Colca;[b] Timothy T. Parker;[c] Gerald D.Artman III;[c,d] Scott D. Larsen;[e] William G. McDonald;[b] Robert C. Gadwood;[c] Rolf F. Kletzien;[b] James B. Zeller;[f] Pil H. Lee,[e] Wade J. Adams[g]

a) SPTanis PharmaChem Consulting LLC, Carlsbad, CA 92011; b) Metabolic Solutions Development Co., Kalamazoo, MI 49007; c) Kalexsyn, Kalamazoo, MI 49008; d) Current address: Celgene, Summit, NJ 07901; e) Vahlteich Medicinal Chemistry Core, University of Michigan, Ann Arbor, MI 48109; f) Jim Zeller Consulting, Scottsdale AZ 85259; g) ADaMET Consulting LLC, Kalamazoo, MI 49008

Declaration of Interest: JRC, WGM, RFK have an interest in Metabolic Solutions Development Co.

1. INTRODUCTION

Insulin sensitizers, particularly pioglitazone, are among the most useful treatments for type 2 diabetes as they correct the key feature of the disease and exert durable actions not only restoring the action of peripheral tissues to insulin but also preserving the function of pancreatic beta cells that produce and secrete insulin. Unfortunately, the mechanism of action of these molecules has been poorly understood and no new insulin sensitizers have been approved for clinical use since pioglitazone in 1999.[1] It has become generally accepted that the transcription factor PPARγ is the direct molecular target for these molecules even though pioglitazone, the weaker PPARγ activator of the two remaining thiazolidinediones (TZDs; pioglitazone and rosiglitazone) has the clinically improved therapeutic activity *vs* rosiglitazone and PPAR directed efforts have yet to yield a new TZD or a new class of insulin sensitizer with market approval. We have suggested that an alternate approach to this problem might be to go 180 degrees away from this PPAR driven paradigm and to examine the impact of a minimization of the direct interaction with PPARγ while maintaining activity with the recently identified mitochondrial target of these molecules.[2] This approach has given rise to two new analogs in clinical development[3] and to the identification of the mitochondrial target as the mitochondrial pyruvate carrier. This work suggests that the transcriptional networks are downstream of a metabolic event and thus might reconcile the importance of the transcription networks to some of the pharmacology of the TZDs and the fact that direct activation of these networks may not be a key feature of a successful drug candidate.[4] Here we describe the

medicinal chemistry approach to design away from the direct activation of PPARγ that was employed in an attempt to improve on structures which had previously demonstrated clinical effectiveness.

A short history of the background endeavors, which we have previously reviewed (*vide infra*), is presented here. The original biological analyses for all of the initial TZD analogs was done in diabetic animal models as pioneered by Sohda, Ikeda, Fujita and colleagues at the Takeda company in the 1970s.[5] These compounds were found to lower both circulating glucose and insulin and they came to be known as insulin sensitizers.[6] The Takeda analogs, ciglitazone **1** (Figure 1) followed by pioglitazone **2** moving first into clinical trials, however troglitazone **4**, an analog synthesized by Sankyo, was the first compound from this class (as Rezulin®) approved for the market in 1997. This was followed by the approval of rosiglitazone **3** (as Avandia®) and then pioglitazone **2** (as Actos®) in 1999.[7] The PPARγ IC_{50} numbers shown in Figure 1 were determined years after the selection of these compounds for development as the identification of this transcription factor as a binding site came some 10 years after the selection of the only three compounds with this action to be approved and marketed to treat type 2 diabetes. The conclusion that peroxisome proliferator-activated receptor γ (PPARγ) was the direct target of these molecules was primarily based on the activity of the most potent activator of this original group of compounds, rosiglitazone **3**.[8] The conclusion that PPARγ was the relevant target was bolstered by the ability to find other compounds that activated PPARγ and which were also active as insulin sensitizers.[9]

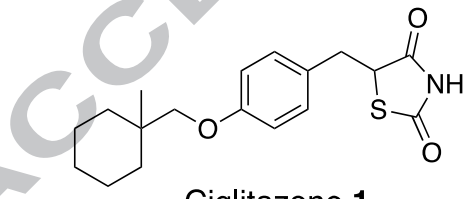

Ciglitazone **1**
PPARγ IC_{50} = > 5μM

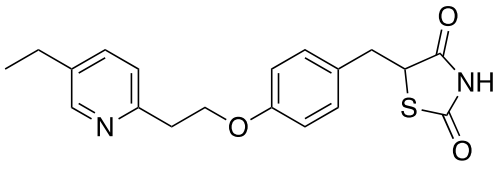

Pioglitazone **2**
PPARγ IC_{50} = 1.79μM

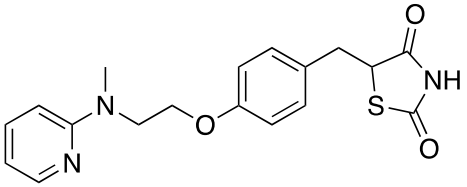

Rosiglitazone **3**
PPARγ IC_{50} = 0.112μM

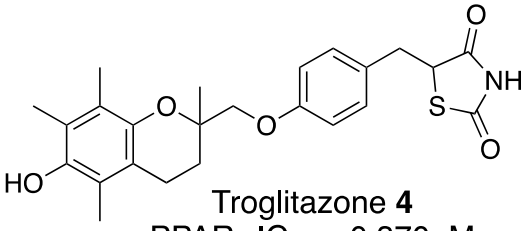

Troglitazone **4**
PPARγ IC_{50} = 0.370μM

Figure 1: Initial thiazolidinedione insulin sensitizers- discovered though whole animal assays

Once troglitazone **4** was removed from the market because of a unique idiosyncratic hepatotoxicity, a concerted effort was made to expand out of this chemical class using rosiglitazone **3** and related analogs as templates in an effort to find new PPARγ agonists. These efforts resulted in the discovery of many other TZD and related molecules that have entered into development, although none of these compounds has achieved market approval.[10,11,12] The primary intent of these later chemical programs was to increase potency, specifically, designing toward more potent and/or more selective direct activation of PPARγ.[13] Again, it must be noted that the marketed clinical candidates were selected 10 years before the PPARγ hypothesis was developed.

Figure 2 shows that the starting point for many of the non-TZD clinical candidates that came from industry programs was a Takeda compound AD-5075, one of the most potent analogs from the original medicinal chemistry approach in terms of ability to stimulate the differentiation of adipocytes.[14] Potent PPARγ agonists were created by replacing the TZD ring with other acidic bioisosteres (the calculated pKa of the majority of the isosteres ranged between 6.4 for TZDs to 3.6 for alkoxy acids), with most of the efforts keeping the left-hand portion of the molecule fairly constant, while deleting the OH-from the linker.[15-20] Some of these changes resulted in analogs that bear resemblance to the fibrates (which are known as PPARα agonists) that also activated other nuclear receptors from the PPAR family. These have included compounds that affect some (γ, α, or γ+α) or all (γ, α, δ) of the PPAR-related nuclear receptors.[21] The one constant for both the newer TZDs and the non-TZDs that have failed (summarized on the right side of Figure 2) is that they were all designed with the ides of activating PPARγ and then particularly with the non-TZDs, other members of the PPAR class.

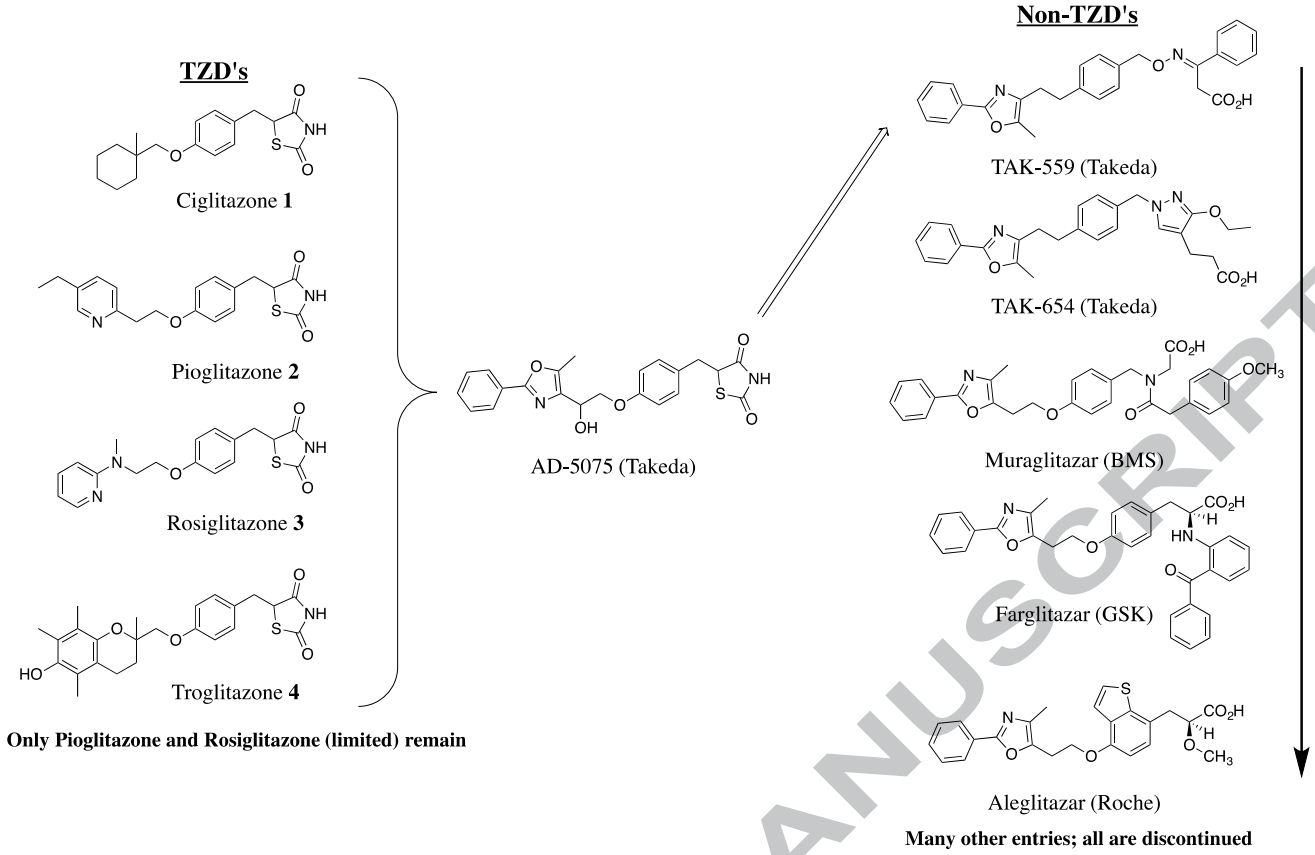

Figure 2: Insulin sensitizer families. Ciglitazone was the first insulin sensitizer tested in clinical trials. Troglitazone, rosiglitazone, and pioglitazone are the only insulin sensitizers ever to be approved for treatment of type 2 diabetes. Representative non-TZDs are shown on the right side of the page. Most of these compounds were modeled after Takeda's AD-5075, which was the most potent of the original Takeda analogs at differentiating 3T3L1 preadipocytes,[14]each with various replacements for the TZD ring. None of these compounds have been approved in the major markets.

The case for a prominent role of PPARγ as a mainstay of the pharmacology was made mostly from study of the differentiation of adipose tissue. However, the pleitropic insulin sensitizing pharmacology of the thiazolidinediones cannot be solely explained by action on preadipocytes and the expansion of white fat[22a,b,c]as TZD's still exert some actions in animals wherein white fat has been eliminated.[22d] There are effects of these compounds on multiple cell types that cannot be solely attributed to the direct stimulation of PPARγ, a transcription factor which drives the synthesis and storage of lipids primarily in adipose cells. There is also little

doubt that the weight gain and fluid retention, the main side effects that have limited the use of pioglitazone and rosiglitazone, are clearly due to PPARγ agonism.

As we have reviewed elsewhere, the limited success of these abovementioned endeavors might be due to the focus of all research activities on the wrong target(s).[22c] There is evidence that a considerable portion of the insulin-sensitizing effect might involve anti-inflammatory or direct metabolic actions, including those in the mitochondrion.[22b] It should also be pointed out that recent evidence from long-term trials has suggested that of the two TZDs currently in clinical use, the weaker of the PPARγ activators, pioglitazone **2**,[2,23] has significant advantages over the stronger activator, rosiglitazone **3**, in practice (Figure 1).[24-26] This includes recent evidence that long-term treatment with pioglitazone might prevent both dementia[27a] as well as favorably affect cardiovascular outcomes including heart attacks and stroke.[27b,c] These findings together with the failure of multiple efforts to successfully develop structurally diverse, potent PPAR activators for the treatment of diabetes support the view that a diminution of direct chemical activation of this transcription factor should be pursued.[22c] This hypothesis can be more directly tested with a series of TZDs that avoids binding to PPAR transcription factors. If this hypothesis is correct, insulin-sensitizing pharmacology as well as other pleiotropic effects of TZDs could result from defined, direct action on non-PPAR targets and this should allow the insulin-sensitizing pharmacology to be unencumbered by PPAR-related side effects.

As we have described elsewhere, evidence has been accumulating suggesting, that TZDs have direct effects on the mitochondria from various types of cells.[22a, 28] Labeling studies with tritiated pioglitazone[29a] and a photoaffinity pioglitazone-analog[29b-c]led to proteins in the inner mitochondrial membrane which were initially called the mitochondrial target of thiazolidinediones (mTOT). Further studies resulted in the identification of these proteins as the mitochondrial pyruvate carrier (MPC), composed of two proteins MPC1 and MPC2 in the inner mitochondrial membrane.[30a-c] This complex is required for pyruvate to enter the mitochondrial matrix, where it is metabolized, from its site of synthesis in the cytosol. Recent efforts have suggested targeting MPC for treatment of a variety of metabolic and inflammatory diseases, including diabetes,[23, 31] Parkinson's and other

neurodegenerative diseases,[32] and nonalcoholic fatty liver disease (NAFLD).[30a, 33]

Recent reports have suggested that the alteration of carbon flow through the pyruvate carrier results in changes in carbon flow from other sources[31b, 34a,b] in order to construct requisite building blocks, which has implications with respect to the delivery of substances to key cellular regulatory machinery.[34c] These entities are the executors of post-translational regulation of proteins and the subsequent epigenetic regulation of gene expression. TZD treatment and the impact that these compounds have on metabolism thus results in the differentiation of stem and progenitor cells.[35] Another important aspect to consider in the discussion of the pharmacology of the TZDs *in vivo* is that significant efficacy only occurs in metabolically challenged animal models which are insulin resistant, either genetically, or by co-treatment with drugs or hormones (*e.g.* glucocorticoids, growth hormone) or with diets/agents which cause insulin resistance.[7, 22b] Therefore, it appears that the effect of TZDs is to reduce insulin resistance rather than to increase insulin sensitivity *per se*, making it difficult to study the effects of TZDs on isolated cells in culture.

As it is generally accepted that excess calories can help predispose to insulin resistance and type-2 diabetes, and weight loss and reduction of caloric intake can protect against even moderate diabetes, it is likely that the precipitation of the diabetic state involves a plethora of systems that are regulated by the availability of nutrients. Nutrient sensing mechanisms such as AMPK and the mTOR complexes coordinate downstream and parallel control points of gene expression, and TZDs are known to impact these processes. In many systems, treatment with TZDs has been shown to result in both activation of AMPK and reduction of the activity of mTORC1.[35] The precise mechanistic details of this effect remain to be elucidated, however one could imagine that selective signals could be generated as a function of the relative amount of pyruvate that enters through the facilitated carrier vs. the alternate delivery of substances, and that the understanding of these downstream events will afford important insights into treating metabolic disease. With this understanding, in 180 degree opposition to the prevailing hypothesis, we sought to reduce the direct interaction of new analogs with PPARγ.

The initial design criteria that informed this effort to reduce the direct activation of PPARγ was provided by a simple two-dimensional overlay of the key thiazolidinediones **1** – **4** (Figure 3). The shortest backbone is associated with ciglitazone **1** (red) which also is the least effective PPARγ activator (IC_{50} >5μM). The next longest backbone extension is exhibited by pioglitazone **2** (PPARγ IC_{50} = 1.79μM) with rosiglitazone **3** (PPARγ IC_{50} = 0.112μM) and troglitazone **4** (PPARγ IC_{50} = 0.370μM) pushing relatively lipophilic aryl rings further from the thiazolidinedione head group than **2**. This extension of planar lipophilicity appeared to be of some significance with respect to PPARγ activity, but it seemed to be abrogated by the presence of polarity in the vicinity of the lipophilic terminus.

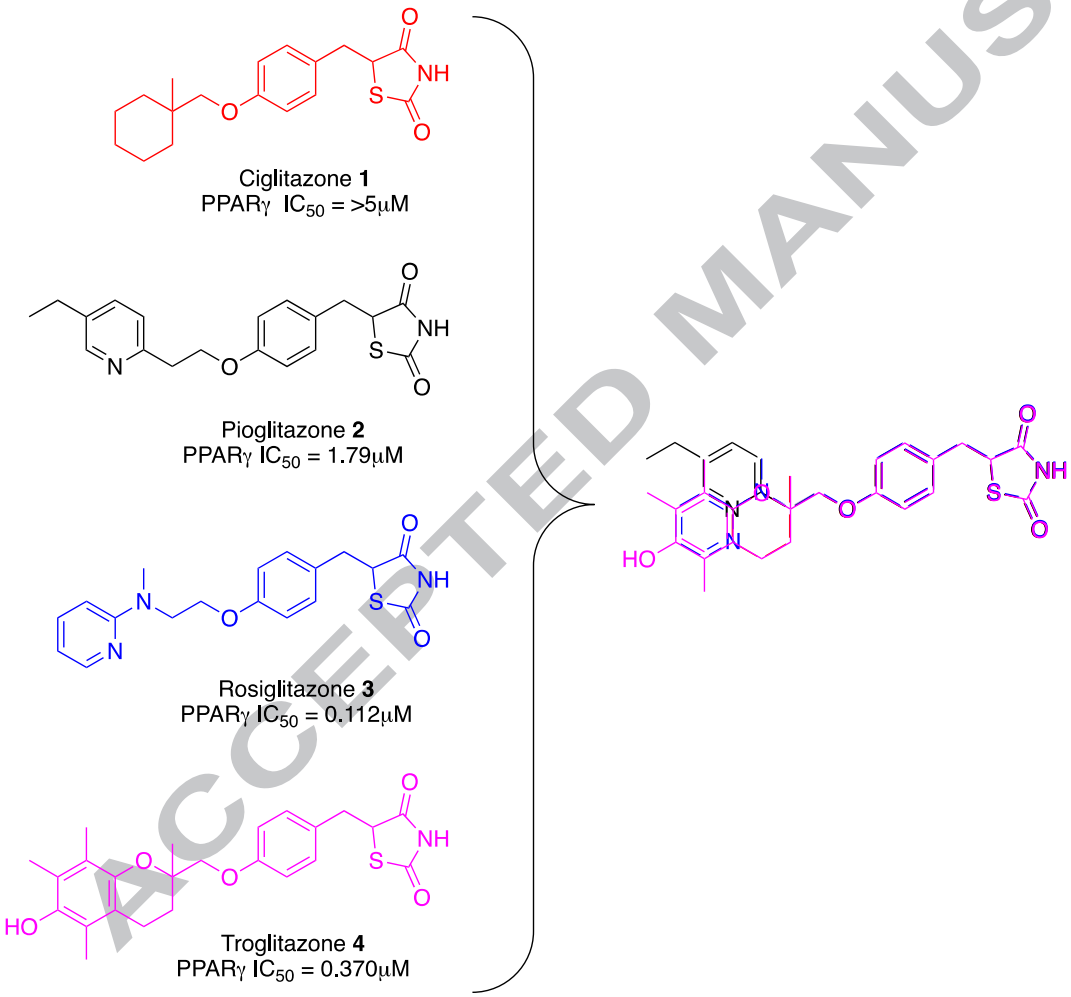

Figure 3: 2D Overlays of Glitazones **1** - **4**

If we compare the 2D overlay of pioglitazone **2** (PPARγ IC_{50} = 1.79μM) with muraglitazar **5**[36] (PPARγ IC_{50} = 120nM) we see (Figure 4) an extension of lipophilicity beyond that associated with rosiglitazone **3** or

troglitzaone **4** with an imperfect overlay of the acid moiety with the TZD. In the case of muraglitazar **5** a PPARγ IC_{50} = 120nM does support the notion of the impact of backbone length and lipophilicity of PPARγ IC_{50} values.

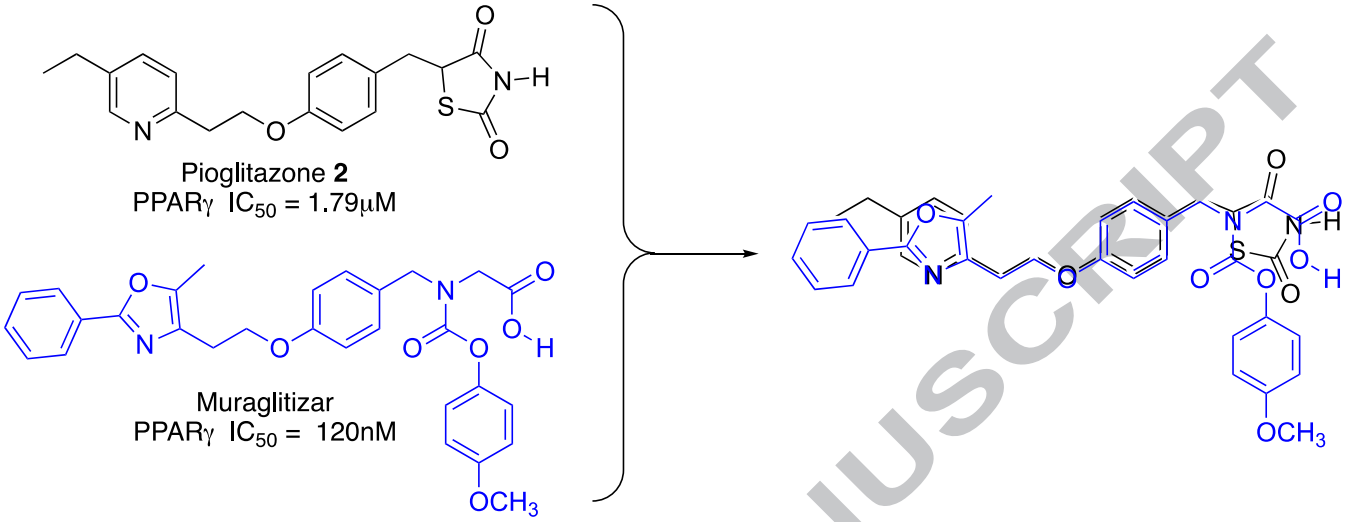

Figure 4: 2D Overlay of a TZD – Pioglitazone **2** with a non-TZD Muraglitazar.

As a result of the general SAR discussed above (*vide supra*) we elected to consider the preparation of thiazolidinediones of the same relative backbone length as that of pioglitazone with polarity near the terminus in the form of the pyridine-N and a proximal C=O or CH-OH as well as a benzene ring, alkyl- or alkoxy-substituted and with a proximal C=O or CH-OH. These entities would be limited in number and in relatively close physicochemical space to an entity, pioglitazone **2**, of clinical interest / importance. These notions would allow us to further examine the impact of polarity near the terminal aromatic ring as well as the potential for asymmetry, in the form of the CHOH, to alter the PPARγ IC_{50}. This led us to design the series of 12 molecules (**5-16**) shown in Figure 5 below. The ketone targets are presented in descending order of their c-LogD values.[37]

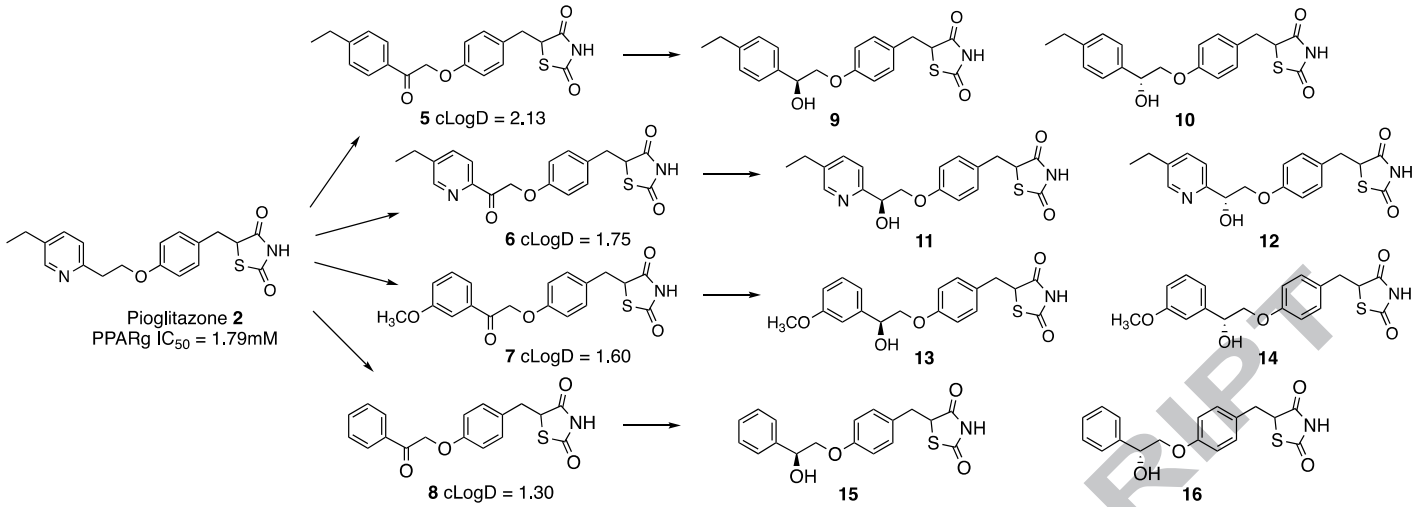

Figure 5: Targets **5 – 16** Designed to Examine the Impact of Polarity on PPARγ and Antidiabetic Activity

2. CHEMISTRY

We had previously reported the synthesis of **6**[38]starting from Pioglitazone **2**. Of note in that endeavor, was the difficult oxidation of the carbinol precursor of **6**.[38,39] Ketone **8** was then targeted using a styrene oxide approach (Scheme 1)[40] developed during a process chemistry evaluation of the synthesis of **6**.[41] This initial epoxide ring opening reaction encountered similar selectivity issues as had been described[40] and a somewhat lower yield was realized. Exposing styrene oxide to the phenoxide prepared from 4-hydroxybenzaldehyde in a toluene / PEG4000 mixture led to a 1.8:1 mixture of **20**:**19** with **20** isolated in 34% yield. In the case of the pyridyl based epoxide[40] a ca. 4:1 ratio of primary *vs* secondary attack was realized with the desired material comprising ca. 80% of the mixture. Clearly, this styrene oxide system performed differently, suggesting the need for alternate approaches to **5** and **7**.

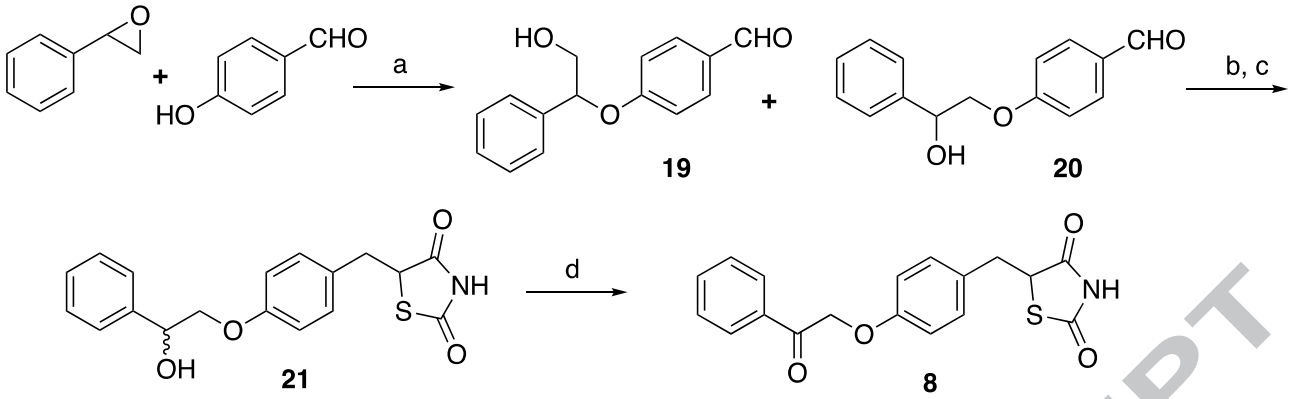

Scheme 1. (a) PEG4000, 1M aq. NaOH, toluene 80°C, 34% [**20**]; (b) 2,4-thiazolidinedione, piperidine, abs, EtOH Δ, 86%; (c) $CoCl_2$-6-H_2O, dimethylglyoxime, 1M aq. NaOH, aq. $NaBH_4$ (in 0.2M aq. NaOH), 76%; (d) DMSO, P_2O_5, Et_3N, CH_2Cl_2 (40%).

With **20** in hand we continued our efforts toward **8** (Scheme 1) as we have previously reported.[38] Condensation between **20** and 2,4-thiazolidinedione, mediated by piperidine, gave the expected Knoevenagel product (86%), which was smoothly reduced using the modified conjugate reduction protocol ($CoCl_2$-$6H_2O$, dimethylglyoxime, $NaBH_4$)[38] to give racemic alcohol **21** (76%). Application of the Taber[39] oxidation conditions[38] to **21** did lead to the desired **8**, albeit in a disappointing 40% yield.

Our next target, the 4-ethyl-substituted ketone **5**, (Scheme 2) would serve as the test case for direct ketone introduction and an examination of overall yield for the redox cycle at that center required as a result of the chemistry utilized for the conjugate reduction of the methylene-2,4-thiazolidinedione bond. In the event the known bromide (R_1 = CH_2CH_3, R_2 = H was readily reacted with 4-hydroxybenzaldehyde (K_2CO_3, acetone) to afford aldehyde **22a** (61%). Knoevenagel condensation (2,4-thiazolidinedione, piperidine) afforded **23a** (55%) which, when exposed to conjugate reduction accomplished with 2,2'-bipyridine as the cobalt ligand, led to the expected doubly reduced alcohol **24a** (76%). Application of the Taber oxidation conditions to this ethyl substituted benzylic alcohol resulted in and a 72% yield of ketone **5**. The overall yield of **5** as shown in Scheme 2 was a modest 18%.

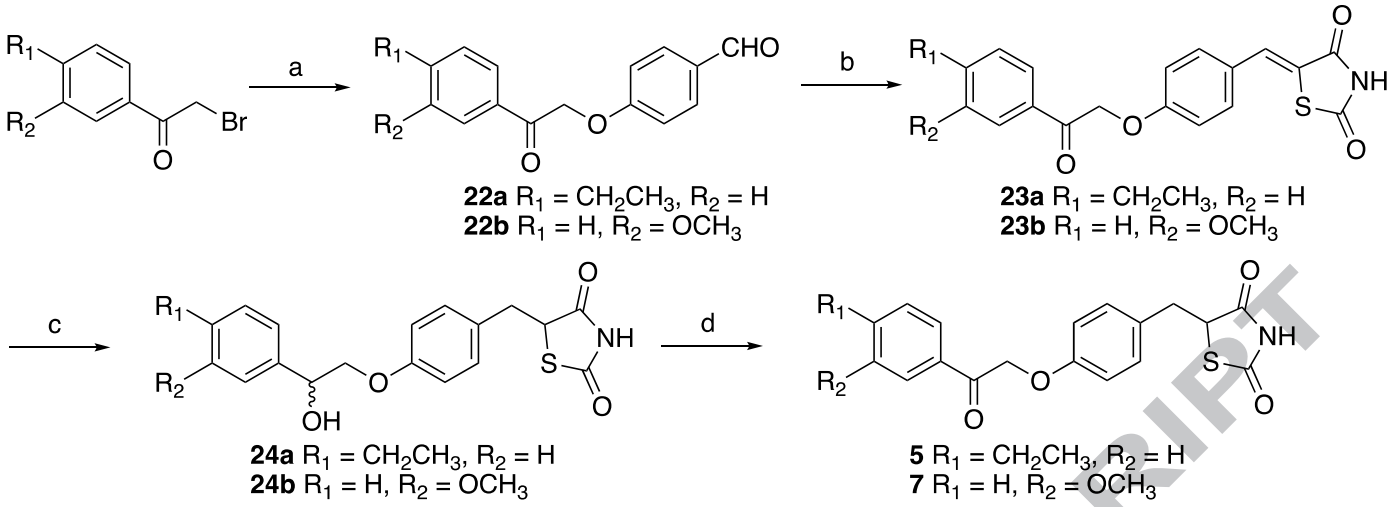

Scheme 2. (a) 4-hydroxybenzaldehyde, K_2CO_3, acetone, **22a** 61%, **22b** 62%; (b) 2,4-thiazolidinedione, abs. EtOH, piperidine, Δ, **23a** 55%, **23b** 76%; (c) $CoCl_2$-$6H_2O$, 2,2'-bipyridine, 1N aq. NaOH, $NaBH_4$ **24a** 76%, **24b** 85%; (d) from **24a** P_2O_5, DMSO, *i*-Pr_2NEt, CH_2Cl_2, **5** 72%; from **24b** IBX, EtOAc, Δ, **7** 77%.

The final ketone target **7** was prepared as shown in Scheme 2. Commercially available 3-methoxy-phenacyl bromide was coupled with 4-hydroxybenzaldehyde to give **22b** (62%) and Knoevenagel condensation then furnished **23b** (76%). Conjugate reduction and concurrent ketone reduction then led to alcohol **24b** in a reasonable 85% yield. Benzylic alcohol oxidation was accomplished with IBX (refluxing EtOAc) to yield ketone **7** (77%). IBX had been examined during the extensive oxidation studies of Scheme 1[38] and again during the process evaluation[41] to no avail in that pyridyl system. The direct ketone introduction, redox paradigm of the oxidation modification noted in Scheme 3 did provide **7** in a somewhat improved 31% yield when compared with the Scheme 3 results leading to **5** wherein the Taber oxidative paradigm was employed.

3. RESULTS AND DISCUSSION

With our target ketones **5-8** in hand we planned to allow their evaluation *in vitro* and *in vivo* inform us with respect to those ketones which might then be selected for chiral reduction to alcohols such as those depicted in Figure 5. Ketones **5-8** were first examined in a PPARγ TR-FRET competitive binding assay[42a] using rosiglitazone **3** as the positive control which was employed to measure binding affinity for PPARγ. All of the

ketones of Table 1 show diminished PPARγ binding affinity when compared to pioglitazone **2**. Pioglitazone derived **6**[38] (PPARγ IC_{50} = 22.30μM) and methoxy-aryl ketone **7** (PPARγ IC_{50} = 18.14μM), shifted ca. 13X and 10X from **2** respectively, exhibited the poorest PPARγ binding affinity. Thus, ketones **6** and **7** were selected for *in vivo* evaluation[38, 43] of antidiabetic activity in the obese, hyperglycemic, hyperinsulinemic, KKA^y mouse.[43d] Animals were grouped into treatment and control groups through pre-test blood glucose measurements and treatment groups had ketones **6** and **7** administered as a food admixture at 100mg / kg / day for 4 days.[43d] The glucose level for the treated group (T) over the control group (C) was used to determine the antihyperglycemic activity and the results are reported as a T/C value. This is computed by the ratio of the terminal glucose level of mice that have undergone 4 days of treatment with the experimental compound divided by the average glucose level of the control group given the vehicle control for the study. A compound with a T/C value ≤ 0.85 is considered active in this model of diabetes. Pioglitazone **2** (100mg / kg) served as the positive control. Pioglitazone **2**, the positive control lowered blood glucose in the KKA^y mice providing a T/C = 0.56. Ketones **6** and **7**, which exhibited 12.5X and 10X poorer PPARγ binding selectivity than **2** were fully effective as antihyperglycemic agents and were associated with T/C values of 0.52 and 0.58 respectively.

Table1: PPARγ Binding Activity (IC_{50}) and Antihyperglycemic Activity of Ketones **5-8**

Compound	PPARγ IC_{50} (μM)	KKA^y T/C
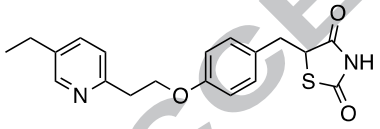 Pioglitazone **2**	1.79	0.56
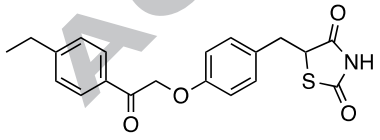 **5** cLogD = 2.13	8.46	NT
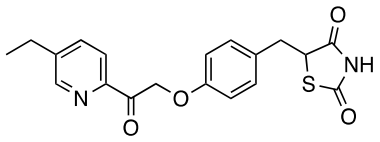 **6** cLogD = 1.75	22.30	0.52

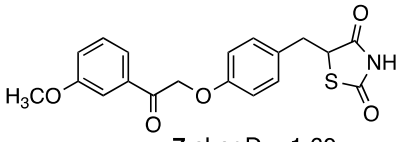 **7** cLogD = 1.60	18.14	0.58
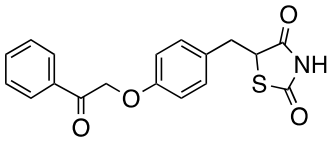 **8** cLogD = 1.30	11.70	NT

The data of Table 1 suggested that ketones **6** and **7** would serves as appropriate substrates for conversion into the respective enantiomeric alcohols **11**, **12** and **13**, **14** (Figure 5) for evaluation of this change in polarity and the presence of asymmetry near the terminus on PPARγ binding and antihyperglycemic activity. Toward that end **6** and **7** were reduced using our previously reported modified Noyori conditions[44] as shown in Scheme 4 to afford alcohols **11**, **12**, **13**, and **14** in good to excellent yields (85-98%) and excellent enantiomeric excess at the carbinol center (96%ee). We were not concerned about the asymmetric center at the 5-position of the thiazolidinedione moiety as it has been demonstrated to readily racemize *in vivo*.[43c]

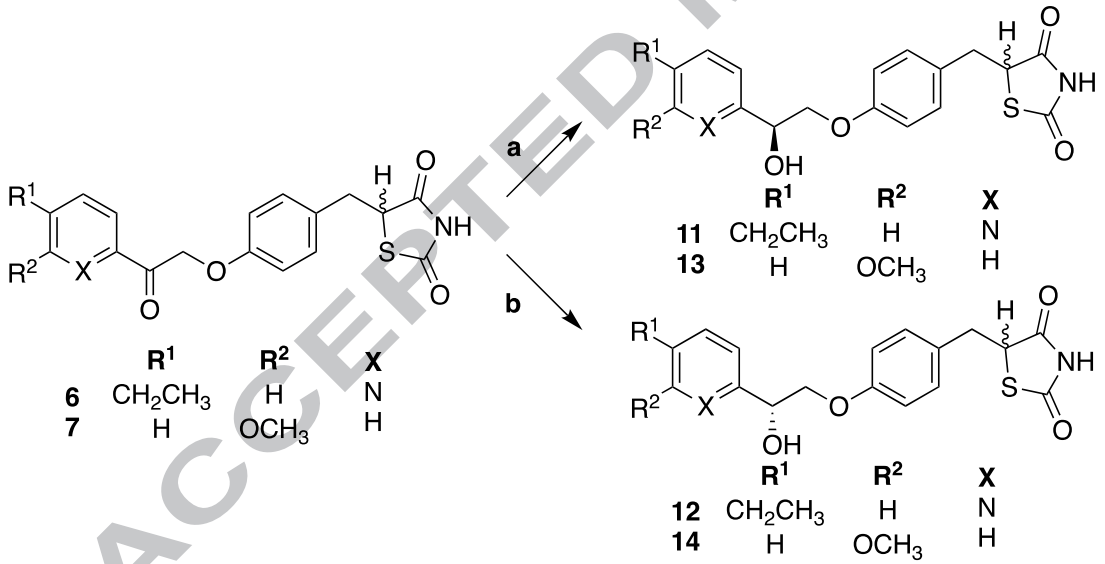

Scheme 3: (a) i. dichloro(η^6-*p*-cymene)ruthenium(II) dimer, (1*R*, 2*R*)-(-)N-p-tosyl-1,2,diphenylethylenediamine, *i*PrOH, Δ; ii. **6**, HCOOH/Et_3N, 85%, 96%ee; **7** 98%, 96%ee; (b) i. dichloro(η^6-*p*-cymene)ruthenium(II) dimer, (1*S*, 2*S*)-(+)N-p-tosyl-1,2,diphenylethylenediamine, *i*PrOH, Δ; ii. **6**, HCOOH/Et_3N, 90%, 96%ee; **7** 96%, 96%ee.

Table 2 presents the data associated with rosiglitazone **3**, pioglitazone **2**, ketones **6**, and **7** as well as the related enantiomeric alcohols **11**, **12**, **13**, and **14** gathered in the aforementioned *in vitro* PPARγ binding assay (IC_{50})[42a], the PPARγ direct transactivation-agonist assay (EC_{50})[42b], as well as the antihyperglycemic activity (T/C) as measured in the KKA^y mouse model.[38,43] Starting from the benchmark compounds rosiglitazone **3** and pioglitazone **2**, the aforementioned binding affinities (**3** IC_{50} = 0.112μM; **2** IC_{50} = 1.79μM) illustrate that rosiglitazone **3** is a ca. 16X better PPARγ binder than pioglitazone **2**. Although the absolute values for EC_{50} - IC_{50} differ in the transactivation assay as compared to the binding assay, the relative differential potencies of the compounds mirrored fairly well in the PPARγ direct transactivation-agonist assay with **3** exhibiting an EC_{50} = 0.008μM while pioglitazone is associated with EC_{50} = 0.098μM, a >12X differential. Both **3** and **2** are fully effective as *in* vivo antidiabetic agents with KKA^y T/C values of 0.55 and 0.56 respectively. Ketones **6** and **7** are poorer PPARγ binders than **3** and **2** (**6** 200X *vs* **3**; >12X *vs* **2**; **7** 162X *vs* **3**, 10X *vs* **2**). The PPARγ transactivation-agonist activity EC_{50} values measured for **6** (EC_{50} = 0.657μM) and **7** (EC_{50} = 0.961μM) are shifted ca. 7-10X *vs* **2** and 80-100X *vs* **3**. As mentioned previously (Table 1), ketones **6** and **7** exhibit good antihyperglycemic activity (T/C = 0.52, 0.58 respectively), equivalent to that of **3** and **2**. The impact of chiral reduction on the PPARγ binding activity (IC_{50}) and PPARγ transactivation-agonist activity (EC_{50}) of the alcohols thus formed is both interesting and surprising. The physicochemical space occupied by ketone *vs* alcohol as determined by the cLogD value changes little for the pyridyl system (**6** cLogD = 1.75; **11**/**12** cLogD = 1.87), and alters to a greater extent for the phenyl congeners (**7** cLogD = 1.60; **13**/**14** cLogD = 1.16). The magnitude of these changes might be expected to have a minor effect on the PPARγ binding activity, however as is obvious from the data of Table 2, asymmetry at the carbinol center has a very large impact on PPARγ binding IC_{50} and PPARγ transactivation-agonist EC_{50} values. The reduction of the carbonyl of ketone **6** to *S*-alcohol **11** results in a >7x shift in binding activity (**6** PPARγ IC_{50} = 22.30μM to **11** PPARγ IC_{50} = 3.12μM) toward stronger binding and a 2.4X shift toward greater activity in the PPARγ transactivation-agonist assay (**6** EC_{50} = 0.657μM to **11** EC_{50} = 0.271μM) while reduction to the *R*-alcohol **12** has the opposite impact shifting toward weaker PPARγ binding affinity (**12** PPARγ IC_{50} = 50.14μM) a shift of more than 16-fold **12** *vs* **11**, and a

2.6X shift toward poorer PPARγ transactivation-agonist activity (**6** EC_{50} = 0.657μM, **12** EC_{50} = 1.74μM). Similar carbinol impacts are observed for the *S*-alcohol **13** (PPARγ IC_{50} = 2.32μM; PPARγ EC_{50} = 0.172μM) derived from **7** (PPARγ IC_{50} = 18.14μM; PPARγ EC_{50} = 0.961μM) while the *R*-alcohol **14** is shifted some 34-fold toward weaker binding / ca. 2X shift toward poorer transactivation-agonist activity, exhibiting very little binding affinity (**14** PPARγ IC_{50} = 78.45μM) and lesser transactivation-agonist activity (PPARγ EC_{50} = 1.72μM). As this progression from alkane to ketone to *R*-alcohol has resulted in successively poorer PPARγ binding / lower PPARγ transactivation-agonist activity we would expect a corresponding falloff in antihyperglycemic activity, as measured by the KKA^y mouse T/C if PPARγ binding and agonist activity were critical for blood glucose lowering *in vivo*. Ketones **6**, **7** and alcohol **12** demonstrated no significant binding to PPARα or PPARδ using GW7647 and GW0742 as positive controls respectively. Full antihyperglycemic activity (Table 2) was still observed for **6, 7**, **12**, and **14**. *Clearly, designing away from potent, direct activation of PPARγ has not been detrimental with respect to antihyperglycemic activity.* Perhaps these data instead implicate the importance of an alternate target, supporting the possible direct effects on the aforementioned mitochondrial target mTOT (*vide supra*) with an impact on pyruvate transport. All of the active compounds were found to compete with the binding of the photoprobe which identified MPC2.[29b] The IC_{50}'s for compounds **6** and **7** to displace the photoprobe from MPC2 are approximately 1.2μM. This is similar to the apparent affinities of the approved diabetes drugs pioglitazone **2** and rosiglitazone **3** in the same assays. Furthermore, all of the active TZD's also slowed the entry and mitochondrial oxidation of pyruvate.[45]

Table 2: PPARγ Binding Activity (IC_{50}), PPARγ Direct Transactivation-Agonist Activity (EC_{50}), and Antihyperglycemic Activity of Pioglitazone **2**, Ketones **7-8**, and Alcohols **11-14**

Compound	PPARγ IC_{50} (μM)	PPARγ EC_{50} (μM)	KKA^y T/C
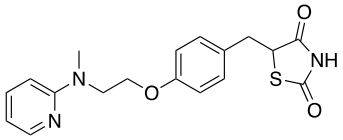 Rosiglitazone **3**	0.112	0.008	0.55

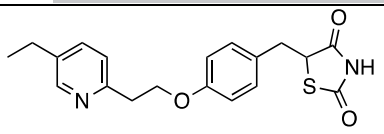 Pioglitazone **2**	1.79	0.098	0.56
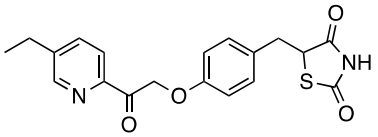 **6**	22.30	0.657	0.52
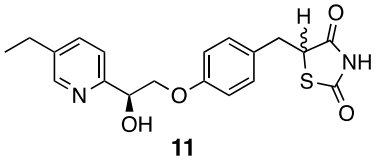 **11**	3.12	0.271	0.54
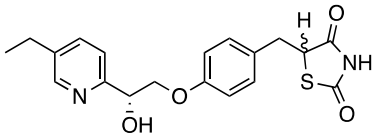 **12**	50.14	1.74	0.56
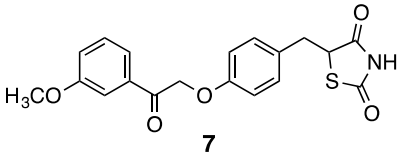 **7**	18.14	0.961	0.58
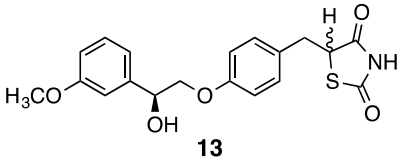 **13**	2.32	0.172	0.53
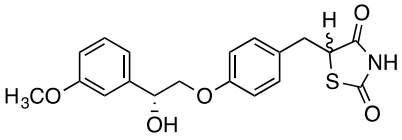 **14**	78.45	1.72	0.65

To rationalize the observed SAR for PPARγ binding affinity of our new analogs several X-ray crystal structures of PPARγ complexed with ligands were examined, and molecular docking studies were carried out using MOE.[46a] There are X-ray crystal structures of the PPARγ ligand binding domain (LBD) with a number of members of the thiazolidinedione (TZD) class of compounds such as lobeglitazone (5y2t.pdb)[47], rosiglitazone **3** (4ema.pdb)[48a], pioglitazone **2** (5y2o.pdb)[47], and rivoglitazone (5u5l.pdb)[48b]. The detailed analyses of PPARγ LBD and its interaction with ligands are described in the literature[47]. In brief (Figure 6), the LBD has a large Y-shaped pocket, which consists of three sub-pockets. The middle pocket is surrounded by mostly nonpolar residues, while the AF-2 pocket, depicted to the right in Figure 6, has a number of polar residues making multiple hydrogen bonds with the TZD head group of ligands, and the pocket at the other end of the Y, the Ω-

pocket, has mainly hydrophobic residues with a few polar residues. When these structures are superimposed, the binding sites near ligands are virtually identical with each ligand binding in a similar fashion. In fact, the TZD in each compound is exactly superimposable, shown bound in the preferred *S*-antipode for the TZD. While the LBD of the nuclear hormone receptors is known to be flexible, the structures of the PPARγ LBD complexed with lobeglitazone, rosiglitazone, pioglitazone, and rivoglitazone are very similar to each other. The root mean square deviations (RMSD) for the Cα atoms of 260 residues of the A chains are 0.58 Å, 0.82 Å, 0.84 Å, and 0.92 Å between complexes with lobeglitazone and pioglitazone, between rivoglitazone and pioglitazone, between lobeglitazone and pioglitazone, and between pioglitazone and rosiglitazone respectively. The structures of the residues within 5 Å from the ligands are more similar. The residues in the middle pocket are very similar, with the exception of F363. The phenyl ring positions of F363 vary slightly, but all remain involved in π-π interactions with the ligand. The E259 and R280 residues, at the end of the Ω-pocket are most flexible, but they are remote with respect to the ligands, rosiglitazone and pioglitazone. The compounds of interest are structurally close to pioglitazone and do not extend to these residues. Rigid as well as flexible docking of ligands were examined, with an induced fit option in MOE, and the docking results were compared with the X-ray structures. Both dockings reproduced the bound conformations of the ligands in the X-ray structures, hence rigid docking was employed. Figure 6 shows a superimposition of pioglitazone **2** (green) and rosiglitazone **3** (magenta) complexed with the PPARγ LBD. The molecular surface of the binding pocket is colored by lipophilicity: hydrophilic in purple and lipophilic in green. Overall, pioglitazone **2** and rosiglitazone **3** bind in very similar fashion and they superimpose very closely through the benzyl-phenyl ring and the oxo-ethyl chain. The two ligands differ at their termini wherein the N-methyl group of rosiglitazone **3** is projected into the lipophilic pocket of the receptor while pioglitazone **2** projects the pyridine nitrogen into this lipophilic pocket. The remainder of the two structures maximize lipophilic interactions with the LBD. We propose that the rosiglitazone **3** N-methyl-lipophilic pocket interaction *vs* the pioglitazone **2** pyridine-N projection into this lipophilic pocket largely accounts for the lower PPARγ IC_{50} of 0.112 μM for rosiglitazone **3** compared to the PPARγ IC_{50} = 1.79 μM of pioglitazone **2**.

Docking studies of 12 compounds, **1-4**, **5-8**, and **11-14**, with PPARγ IC_{50} data into the LBD of PPARγ were carried out using 5y2o.pdb. As described above all of the compounds were bound in the preferred *S*-TZD antipode. The top five docking poses were examined for each and the pose with the best superimposition of the TZD with the pioglitazone **2** crystal structure was selected for comparison. The results from this **1-8** superimposition (not shown) supports the magnitude of the PPARγ IC_{50} data presented in Figure 3 and Table 1 with respect to placement of lipophilic moieties as well as polar groups. Figure 7 presents an overlay of the crystal structure of pioglitazone **2** and the docking pose of ketone **6**. This superimposition suggests that the polar carbonyl group of **6** is projected further into the lipophilic pocket than is the pyridine-N of pioglitazone **2**, which supports the poorer binding IC_{50} = 22.30 μM of compound **6** compared to the data association with pioglitazone **2** (IC_{50} = 1.79 μM). Ketone **7** superimposed with pioglitazone **2**, models similarly (not shown) to the **2** / **6** pairing absent the polar interaction of a pyridine-N but including the projection of the polar carbonyl into the lipophilic pocket, also resulting in reduced PPARγ binding affinity (IC_{50} = 18.14 μM).

The significant eudismic ratio of the antipodal alcohols **11** and **12** is of intense interest and can be readily rationalized from modeling. To that end Figure 8 shows a docking of alcohols **11** and **12** and their superimposition with the crystal structure of pioglitazone **2**. The alcohols superimpose with pioglitazone **2** very well from the TZD-moiety through the alkoxy-ethyl chain. Compounds **2** and **12** have a good concordance of the pyridylethyl portions of the molecule which results in the projection of the polar carbinol-OH into the side wall of the lipophilic pocket. The antipodal *S*-alcohol **11**, however, exhibits a slightly shifted pyridyl ethyl moiety which allows the carbinol-OH to form a strong hydrogen bond with the carbonyl of Leu340. These interactions allow us to rationalize the poorer binding affinity of *R*-alcohol **12** (IC_{50} = 50.14 μM) as well as to understand the stronger binding affinity associated with *S*-alcohol **11** (IC_{50} = 3.12 μM). Modeling performed with alcohols **13** and **14**, superimposed with **2** (not shown) result in a similar conclusion with respect to the poorer binding affinity of *R*-alcohol **14** (IC_{50} = 78.45 μM) as well as the Leu340-H-bond driven improved binding affinity exhibited by *S*-alcohol **13** (IC_{50} = 2.32 μM).

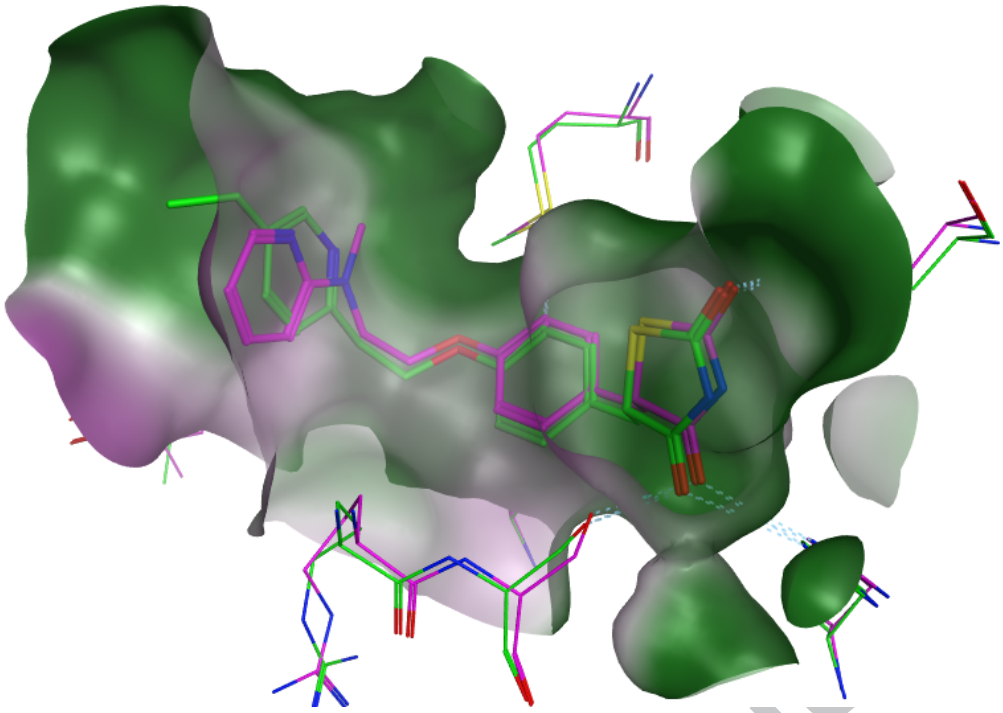

Figure 6: Overlay of crystal structures of pioglitazone **2** (green) and rosiglitazone **3** (magenta) complexed with the LBD of PPARγ. The molecular surface of the binding pocket is colored by lipophilicity: hydrophilic in purple and lipophilic in green.

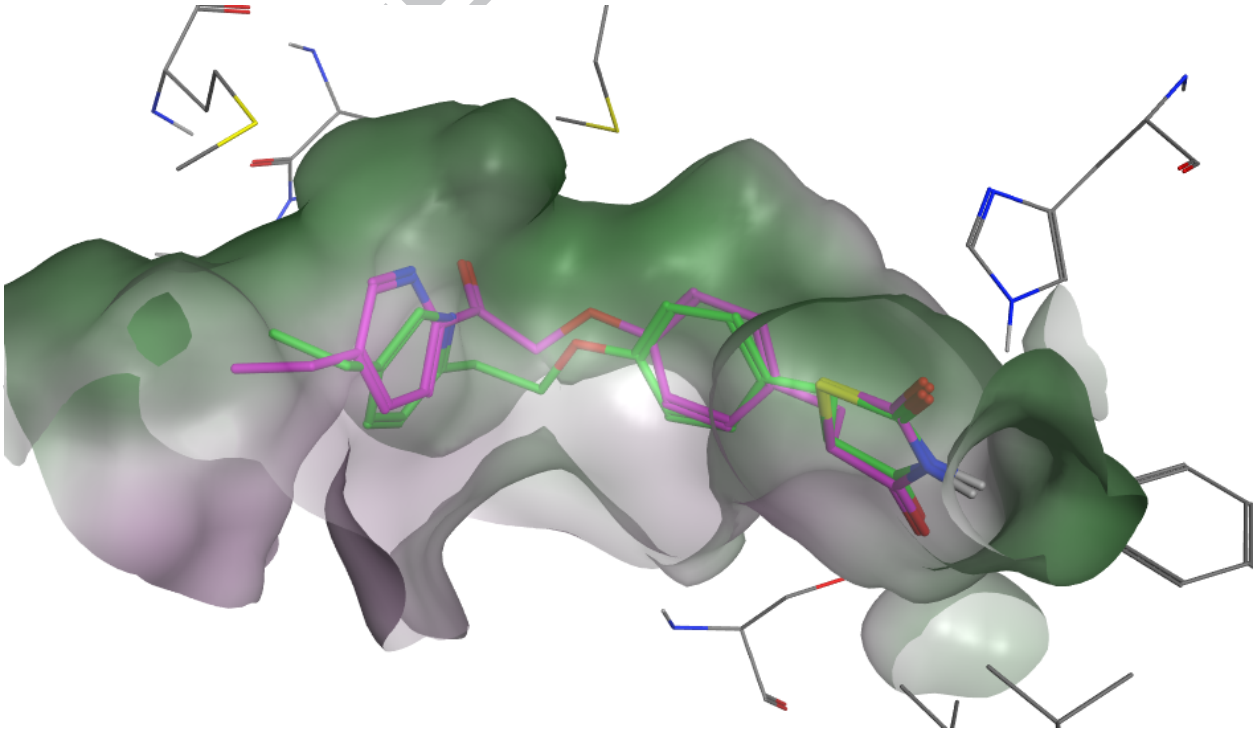

Figure 7: Overlay of the docking pose of ketone **6** (magenta) and the crystal structure of pioglitazone **2** (green).

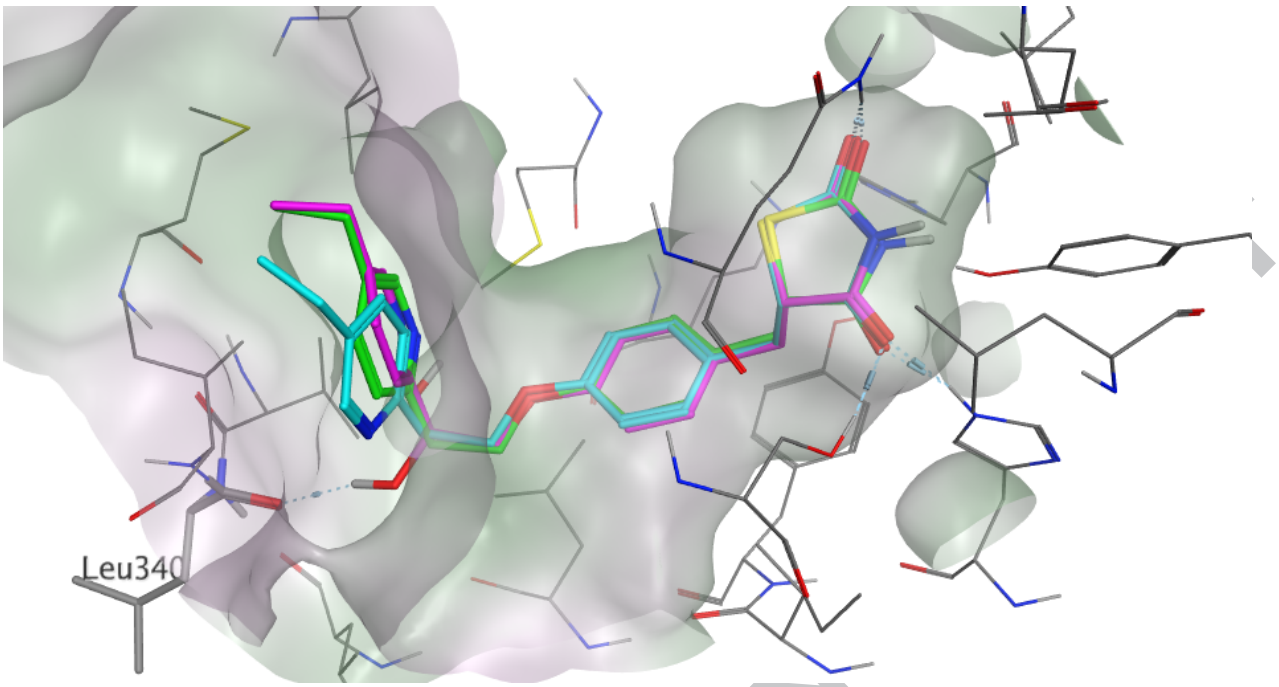

Figure 8: Overlay of docking poses of *S*-alcohol **11** (magenta) and *R*-alcohol **12** (cyan) and the crystal structure of pioglitazone **2** (green). The hydroxyl group of compound **11** is making a hydrogen bond with the carbonyl of Leu340, while the hydroxyl group of compound **12** is turning away from Leu340 into lipophilic pocket.

The favorable characteristics associated with ketones **6** and **7** and the attendant alcohols **12** and **14** spurred us to examine additional properties for **6** and **7** preparatory to possible selection as development candidates. Subsequent metabolism studies (*vide infra*) performed on **6** and **7** would confirm the preferential formation of desired *R*-alcohol metabolites **12** and **14** *vs* the much less desired reductive metabolism to furnish *S* alcohol metabolites **11** and **13**. A collection of *in vitro* and *in vivo* derived data for ketones **6** and **7** is presented in Figure 9.

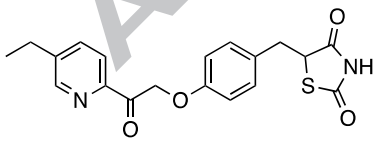

6

PPARγ IC_{50} = 22.30μM

PPARγ EC_{50} = 0.657μM

KKA^{y} T/C = 0.52

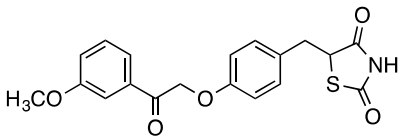

7

PPARγ IC_{50} = 18.14μM

PPARγ EC_{50} = 0.961μM

KKA^{y} T/C = 0.58

hERG IC_{50} >100μM	**hERG** IC_{50} >20μM
CYP2C8 IC_{50} = 26μM	**CYP2C8** IC_{50} = 7μM
CYP2C9 IC_{50} = 22μM	**CYP2C9** IC_{50} = 23μM
hPPB = 99%	**hPPB** = 99%
%F (rat) = 73%	**%F (rat)** = 100%
AMES (+S9) – negative	**AMES (+S9)** – negative
Genotoxicity – not significant	**Genotoxicity** – not significant

Figure 9: Collected *in vitro* and *in vivo* data for ketones **6** and **7**

4. Conclusion

Compounds **6** and **7** are currently progressing through clinical development.[12] Compound **6** was shown to have similar efficacy to 45 mg pioglitazone in a 3 month phase 2b study in diabetic subjects with much less of the PPARγ-related side effects (weight gain and reduction in hematocrit) observed.[31a] Compound **6** was also shown to preserve utilization of glucose in selective brain regions as determined by ^{18}F-2-deoxyglucose PET in subjects with Alzhiemer's disease.[32b] Compound **7** is currently in development for NASH in a 52 week dose ranging trial.[30a] Preclinical studies have shown that unlike direct activators of PPARγ, this compound does not have the same liabilities in terms of stimulating the reabsorption of bone.[40] Also of interest with respect to activation of PPARγ are the metabolic profiles of compounds **6** and **7** found in clinical trials. In the clinic ketone **6** (PPARγ IC_{50} = 22.30μM) was observed to be rapidly reduced to 2 metabolites, alcohols **11** (PPARγ IC_{50} = 3.12μM) and **12** (PPARγ IC_{50} = 50.14μM) in a 10:90 ratio respectively.[31a, 50] Likewise ketone **7** (PPARγ IC_{50} = 18.14μM) was found to be rapidly metabolized *in vivo* to a 14:86 ratio of alcohols **13** (PPARγ IC_{50} = 2.32μM) and **14** (PPARγ IC_{50} = 78.45μM) in humans.[51] As both **6** and **7** were observed to be stereoselectively metabolized in the clinic to the *R*-alcohols **12** and **14**, the shift toward poorer PPARγ metabolite binding and lesser PPARγ residual side effects (*vide supra*) is noteworthy. Compounds **6**[30a, 31b] and **7**[51] together with their major alcohol metabolites **12** and **14** have half-lives *in vivo* from 10-17 hours and have been studied in clinical

trials with once daily dosing. At the clinical doses selected for **6**[30a] and **7**[51] the AUC (area under the curve) observed for **6**[30a] and its major metabolite **12**[30a], as well as the AUC measured for **7**[51] and its major metabolite **14**[51], both bracket the AUC measured for pioglitazone **2** and its active metabolites at a 45mg dose.

We had previously noted (*vide supra*) that designing away from potent PPARγ –binding / transactivation did not result in a detrimental impact in antihyperglycemic activity in the KKA^y mouse model. Of even greater significance is the clinical data associated with ketones **6** and **7** presented above. With this collection of *in vivo* data (murine and human) we have shown, for the first time, that intentionally designing compounds to have minimal PPARγ binding / transactivation activity can be accomplished *without* diminishing *in vivo* antidiabetic activity, while greatly reducing undesired PPARγ side effects. The current evidence indicates that the pharmacology of these molecules is mediated through alteration of the function of the mitochondrial pyruvate carrier in multiple cell types and settings.[29a] More recent efforts have resulted in the preparation of analogs with PPARγ IC_{50} >200μM (binding affinity) and full antihyperglycemic activity in the KKA^y mouse model (T/C = 0.55). These results will be presented in due course.

5. Experimental Section

All reagents were used as received unless otherwise stated. All reactions were performed under a blanket of nitrogen in oven (150°C) dried glassware with rigid exclusion of moisture from all reagents, solvents, and glassware unless otherwise mentioned. Solvents for extraction and purification were of HPLC grade. Chromatographic purification was accomplished using the flash technique of Still *et al*[52] with the following particulars noted: (column diameter in mm OD, quantity of silica gel employed, silica gel mesh) and eluted with the solvents mentioned. Proton magnetic resonance spectra (^{1}H-NMR) were recorded on a Bruker AVANCE 400 spectrometer at 400MHz in the solvent indicated. Chemical shifts are reported in parts per million (δ scale) from internal tetramethylsilane. Data are reported as follows: chemical shifts [multiplicity (s = singlet, brs = broad singlet, d = doublet, dd = doublet of doublets, t = triplet, q = quartet, m = multiplet), coupling constant (Hz), integration]. Most intermediates, and all final compounds were determined to exhibit >95% purity by HPLC. HPLC analyses were performed with an Agilent 1100 HPLC equipped with a Zorbax Eclipse XDB-C18

50 x 4.6mm 1.8 micron column unless otherwise indicated. Solvent A water (0.1% TFA), solvent B acetonitrile (0.07% TFA), gradient 5 min. 95% A to 95% B; 1 min. hold; 1 min. recycle; 30 second hold. UV detection @ 210 and 250 nM with no reference. Mass spectral analyses were performed on a Waters micromass ZQ; Waters 2695 separations module.

Biological Assays

Human PPARγ Competitive Binding: The assay employed a glutathione S-transferase (GST) labelled PPARγ ligand binding domain in combination with a terbium labeled anti-GST antibody and a fluorescent labelled small molecule PPAR tracer ligand. Competitive binding between the unlabeled competitor and the fluorescently labelled PPAR tracer ligand for the nuclear receptor ligand binding site causes a decrease in the FRET signal between the antibody and the tracer. Dose response curves for each test compound were prepared by serial dilutions in DMSO. For the assay, 2X working stocks were prepared from the DMSO stocks in assay buffer over the range from 0.001 to 250μM, resulting in a final DMSO concentration of 1%. Rosiglitazone **3** was employed as the positive control, prepared as above, with a dose response curve from 0.0003 to 30μM. In 384 well polypropylene plates test compound and positive control **3** treated wells received 20 μL of 2X competitor working stock, 10 μL of 4X tracer ligand and 10μL of 4X PPARγ ligand binding domain/terbium labelled anti-GST antibody. The negative control wells received 20μL of 2% DMSO in assay buffer, 10μL of 4X tracer ligand and 10mL of 4X PPARγ ligand binding domain/terbium labelled anti-GST antibody. Each concentration for all concentration groups was assayed in triplicate. The binding interaction was allowed to reach equilibrium by incubating the plate in the dark at 20-24°C for 1 hour. Fluorescence emission was determined on a Bio Tek Synergy 2 plate reader. Two scans were obtained to determine 520/495 ratios. Scan 1 used a 360/40nm excitation filter and a 520/25nm emission filter. Scan 2 used a 360/40 excitation filter and a 495/10nm emission filter. The negative control wells were averaged for background subtraction. IC_{50} values were calculated using a 4-parameter non-linear analysis using Gen5 software (V2.03.1). Dose response curves were generated using Graph Pad Prism software (V5.0).

KKAy Mouse Assay:[2,43d] Groups of 8-12 week old KKAy mice were orally dosed once daily with 30 mg/kg compound for 4 days. The compounds were given as a suspension in 0.1% Tween 80, 1% low viscosity sodium methyl carboxycellulose. Blood glucose was measured after a four hour fast before treatment and 18-20 hours after the last dose. The T/C ratio is the treatment (post 4 days) divided by the initial blood glucose in mg/dL. The number shown is the average for 6 mice.

Human PPARγ Transactivation – Agonist Assay: The GeneBLAzer® PPAR gamma assay uses the ligand binding domain (LBD) of human Peroxisome Proliferator-Activated Receptor-gamma (PPAR gamma) fused to the DNA binding domain (BD) of Gal4 stable integrated into the GeneBLAzer® UAS-bla HEK 293H cell line. GeneBLAzer® UAS-bla HEL 293H cells stable express a beta-lactamase reporter gene under the transcriptional control of an upstream activator sequence (UAS). When an agonist binds to the LBD of PPARγ of the GAL4 DBD-PPAR gamma LBD fusion protein, the protein binds to the UAS, resulting in the expression of beta-lactamase. Florescence Resonance Energy Transfer (FRET) substrate is added to the cells to generate a radiometric dual color (blue/green) reporter signal for both stimulate and unstimulated cells. Rosiglitazone **3** was used as the positive control. Dose response curves for **3** and each test compound were prepared by serial dilutions in DMSO covering a range of 100pm to 25μM with a final DMSO concentration of 0.5%. Each concentration was analyzed in triplicate wells. The frozen GeneBLAzer® UAS-bla HEK 293H cells were suspended in phenol red-free DMEM (Invitrogen #21063-029) containing 2% charcoal stripped FBS (Invitrogen #12676-029) and 100 U/mL penicillin and 100μg/mL streptomycin (Invitrogen #15140-122). 30,000 cells per well in 32μL of medium were transferred into black, clear bottom poly-D-lysine 384 well plates (BD, #354663) and incubated for 2 hours at 37ºC/5% CO_2. Following attachment of the cells, 8μL of assay medium containing 5X drug working stocks were added. Additionally, 8μL of 0.5% DMSO was added to the unstimulated cells as well as the cell free wells. The cells were incubated for 16 hours at 37ºC/5% CO_2, treated with FRET substrate for 2 hours at room temperature in the dark and read on a Biotek Synergy 2 plate reader. Two scans were obtained to determine 460/528 ratios. The first scan used a 400/30 nm excitation filter

and a 528/20 nm emission filter for measuring the green channel. The cell free control wells were averaged for background subtraction of the respective blue and green emission values of the stimulated cells. EC_{50} values were calculated using ma 4-parameter non-linear analysis using Gen5 software (V2.03.1). The dose response curves were drawn using Graph Pad Prism software (version 5.0).

4-(2-Hydroxy-2-phenylethoxy)-benzaldehyde 20: To styrene oxide (6.50g, 54.0 mmol) in toluene (85 mL) was added 4-hydroxybenzaldehyde (9.89g, 81.0 mmol), PEG4000 (polyethylene glycol, 1.15g) and 1M aq. NaOH (85 mL). The mixture was heated in an 80°C oil bath, under nitrogen, overnight. After cooling to room temperature the mixture was poured into EtOAc (250 mL), washed with brine (2 x 250 mL) and dried over anhydrous sodium sulfate. Filtration and concentration *in vacuo* afforded a light yellow oil which was purified by chromatography on silica gel (40 mm OD. 150g 230-400 mesh silica gel) using the flash technique, eluting with 0-10% EtOAc / CH_2Cl_2. A higher R_f (TLC) fraction was isolated (**20**, 4.49g, 34%) and a lower R_f fraction (**19**, 2.46g, 19%) was obtained. Compound **20** was determined to be the desired mode of addition and **19** the regioisomer. Data for **20**: ^{1}H-NMR (400MHz, $CDCl_3$); δ = 9.89 (s, 1), 7.86 (d, J = 8.7 Hz, 2), 7.30 – 7.55 (5), 7.04 (d, H = 8.7 Hz, 2), 5.18 (m, 1), 4.80 (brs, 1), 4.02 – 4.21 (2); MS (ESI+) *m/z* 265.1 (M + Na).

5-[[4-(2-Hydroxy-2-phenylethoxy)phenyl]methylene]-2,4-thiazolidinedione: To a solution of **20** (2.63, 10.8 mmol) in absolute EtOH (75 mL) was added 2,4-thiazolidinedione (1.27g, 10.8 mmol) and piperidine (0.54 mL, 5.4 mmol). The resulting solution was heated to reflux under nitrogen for 10 hours. The mixture was cooled to room temperature, acetic acid (20 drops) was added and the solvent was removed *in vacuo* to give a yellow oil. The crude product was purified by chromatography on silica gel using the flash technique (40 mm OD, 150g, 230-400 mesh), eluted with 30-40% EtOAc-hexanes. Fractions containing the product were combined to furnish 3.18g (86%) of the Knoevenagel product as a pale yellow solid. ^{1}H-NMR (400MHz, DMDO-d_6); δ = 12.53 (s, 1), 7.00-7.80 (9), 5.70 (m, 1), 4.80 (m, 1), 4.02 (m, 2); MS (ESI-) *m/z* 340.1 (M - H).

5-[[4-(2-Hydroxy-2-phenylethoxy)phenyl]methyl]-2,4-thiazolidinedione 21: To a solution of 5-[[4-(2-hydroxy-2-phenylethoxy)phenyl]methylene]-2,4-thiazolidinedione (1.50g, 4.39 mmol) in THF (20 mL) was added H_2O (20 mL), 1M aq. NaOH (3 mL), cobalt (II) chloride hexahydrate (0.60mg, 0.003 mmol) and dimethylglyoxime (15mg, 0.13 mmol). The resulting mixture was treated with a solution of $NaBH_4$ (240mg,

6.33 mmol) in 0.2M aq. NaOH (3.6 mL) over 15 minutes to produce a deep blue-purple color. The pH of the mixture was adjusted to ca. pH 10 during the course of the reaction by the addition of acetic acid. After the reaction was judged to be complete (HPLC) the mixture was cast into EtOAc (250 mL), washed with water (2 x 250 mL), and dried (Na_2SO_4). Filtration and concentration *in vacuo* afforded crude **21** as a foamy, yellow solid. The crude material was purified by chromatography on a column of silica gel using the flash technique (40 mm OD, 150g, 230-400 mesh), eluting with 50% EtOAc-hexanes. Fractions containing the desired **21** were combined and concentrated *in vacuo* to give **21** (1.15g, 76%) as an ivory solid. ^{1}H-NMR (400MHz, $CDCl_3$); δ = 8.00 (brs, 1), 7.20-7.45 (5), 7.17 (d, J = 8.6 Hz, 2), 6.89 (d, J = 8.6 Hz, 2), 5.14 (m, 1), 4.52 (dd, J = 9.3, 4.0 Hz, 1), 3.95-4.10 (2), 3.46 (dd, J = 14.2, 3.9 Hz, 1), 3.14 (dd, J = 14.2, 9.3 Hz, 1), 2.78 (brs, 1); MS (ESI-) *m/z* 342.1 (M - H).

5-[[4-(2-Oxo-2-phenylethoxy)phenyl]methyl]-2,4-thiazolidinedione 8: To a stirring solution of **21** (1.00g, 2.91 mmol) in CH_2Cl_2 (35 mL), cooled in an ice-water bath, was added DMSO (2 mL). Phosphorus pentoxide (0.83g, 2.91 mmol) was added followed by Et_3N (1.8 mL, 13.1 mmol). The reaction was allowed to slowly warm to room temperature and was analyzed by HPLC. When the reaction was judged to be complete the mixture was cast into CH_2Cl_2 (250 mL), washed with water (250 mL), brine (250 mL) and dried (Na_2SO_4). Filtration and concentration *in vacuo* afforded crude **8** as a yellow oil. The crude material was purified by chromatography on a column of silica gel (40 mm OD, 150g, 230-400 mesh) using the flash technique, eluting with 25-35% EtOAc-hexanes. Fractions containing **8** were combined, and concentrated *in vacuo* to furnish 0.40g (40%) of **8** as a white solid. ^{1}H-NMR (400MHz, DMSO-d_6); δ = 12.03 (brs, 1), 8.02 (d, J = 7.2 Hz, 2), 7.70 (m, 1), 7.57 (m, 2), 7.15 (d, J = 8.6 Hz, 2), 6.91 (d, J = 8.6 Hz, 2), 5.56 (s, 2), 4.88 (m, 1), 3.30 (dd, J = 14.2, 4.2 Hz, 1), 3.05 (dd, J = 14.1, 9.3 Hz, 1); MS (ESI-) *m/z* 340.1 (M - H); Anal. Calcd. For $C_{18}H_{14}NO_4S$: C, 63.33; H, 4.43; N, 4.10. Found: C, 63.01; H, 4.28; N, 4.32.

2-Bromo-1-(4-ethylphenyl)-ethanone: To a solution of 1-(4-theylphenyl)-ethanone (6.00g, 40.4 mmol) in acetonitrile (200 mL) was added p-toluenesulfonic acid (10.46g, 60.8 mmol) followed by N-bromosuccinimide (7.20g, 40.4 mmol). The mixture was warmed to reflux under nitrogen and maintained for 2 hours. The mixture was cooled to room temperature, concentrated *in vacuo*, dissolved in CH_2Cl_2 (250 mL), washed with water (2 x

250 mL) and dried (Na_2SO_4). Concentration *in vacuo* afforded the crude bromide as a yellow-brown oil which was purified by chromatography chromatography on a column of silica gel using the flash technique (40 mm OD, 100g, 230-400 mesh) eluted with CH_2Cl_2. Fractions containing the target bromide were combined and concentrated *in vacuo* to afford 8.54g (93%) of 2-bromo-1-(4-ethylphenyl)-ethanone as a pale yellow oil. ^{1}H-NMR (400 MHz, $CDCl_3$): δ = 7.90 (d, J = 8.3 Hz, 2), 7.64 (d, J = 8.3 Hz, 2), 4.48 (s, 2), 2.74 (q, J = 7.6 Hz, 2), 1.27 (t, J = 7.6 Hz, 3).

4-[2-(4-Ethylphenyl)-2-oxoethoxy]benzaldehyde 22a: To a stirring solution of 2-bromo-1-(4-ethylphenyl)-ethanone (2.85g, 12.5 mmol) in acetone (80 mL) was added 4-hydroxybenzaldehyde (1.76g, 14.4 mmol) followed by potassium carbonate (1.99g, 14.4 mmol). The mixture was allowed to stir at room temperature at which point HPLC analysis suggested the reaction was complete. The solvent was removed *in vacuo* and the residue was partitioned between ethyl acetate (125 mL) and water (250 mL). The aqueous phase was extracted with EtOAc (125 mL) and the combined organic layers were washed with brine (250 mL), dried over Na_2SO_4, and concentrated *in vacuo* to afford crude **22a** as a yellow oil. Crude **22a** was purified by chromatography on a column of silica gel using the flash technique (50 mm OD, 150g, 230-400 mesh), eluted with 5-10% EtOAc-haxanes. Fractions containing **22a** were combined and concentrated *in vacuo* to provide 2.07g (61%) of **22a** as an ivory solid. ^{1}H-NMR (400 MHz, $CDCl_3$): δ = 9.91 (s, 1), 7.94 (d, J = 8.3 Hz, 2), 7.86 (d, J = 8.7 Hz, 2), 7.36 (d, J = 8.3 Hz, 2), 7.05 (d, J = 8.7 Hz, 2), 5.40 (s, 2), 2.76 (q, J = 7.6 Hz, 2), 1.29 (t, J = 7.6 Hz, 3); MS (ESI+) *m/z* 269.1 (M + H).

5-[[4-[2-(4-Ethylphenyl)-2-oxoethoxy]phenyl]methylene]-2,4-thiazolidinedione 23a: To a solution of 4-[2-(4-ethylphenyl)-2-oxoethoxy]benzaldehyde **22a** (1.58g, 5.91 mmol) in absolute EtOH (15 mL) was added 2,4-thiazolidinedione (0.761g, 6.50 mmol) and piperidine (0.643 mL), 6.50 mmol). The resulting mixture was warmed to reflux under nitrogen and maintained for 12 hours. The mixture was cooled to room temperature and then in an ice water bath to furnish a precipitate. The solid was isolated by filtration, rinsed with ether, and dried *in vacuo* to give **23a** (1.21g, 56%) as a pale yellow solid. ^{1}H-NMR (400MHz, DMSO-d_6); δ = 12.53 (brs, 1), 7.95 (d, J = 8.2 Hz, 2), 7.75 (s, 1), 7.55 (d, J = 8.7 Hz, 2), 7.42 (d, J = 8.2 Hz, 2), 7.12 (d, J = 8.7 Hz, 2), 5.68 (s, 2), 2.69 (q, J = 7.6 Hz, 2), 1.21 (q, J = 7.6 Hz, 3); MS (ESI+) *m/z* 368.1 (M + H); MS (ESI-) *m/z* 366.1 (M - H).

5-[[4-[2-(4-Ethylphenyl)-2-hydroxyethoxy]phenyl]methyl]-2,4-thiazolidinedione 24a: To a stirring solution of $CoCl_2$-$6H_2O$ (3.36 mg, 0.011 mmol) and 2,2'-bipyridine (70.7mg, 0.45 mmol) in water (16 mL) and THF (16 mL) was added 1.0N aq. NaOH (2 drops) followed by $NaBH_4$ (284mg, 7.5 mmol). The resulting deep blue mixture was cooled in an ice-water bath and a solution of **23a** (0.70g, 1.90 mmol) in THF-DMF (2:1, 12 mL) was added over 0.5 h. The reaction mixture was allowed to slowly warm to room temperature and stir for 18 hours. Acetic acid was slowly added until the pH of the mixture was ca. 6. The mixture was diluted with water (25 mL) and extracted with CH_2Cl_2 (2 x 50 mL). The combined organic extracts were washed with brine (100 mL), dried (Na_2SO_4), filtered and concentrated *in vacuo*. The crude product was purified by chromatography on a column of silica gel using the flash technique (20 mm OD, 30g, 230-400 mesh) eluting with EtOAc-CH_2Cl_2 (1:4). Fractions containing **24a** were combined and evaporated *in vacuo* to give 0.54g (76%) of **24a** as a white solid. ^{1}H-NMR (400 MHz, $CDCl_3$): δ = 7.38 (d, J = 8.0 Hz, 2), 7.25 (d, J = 8.0 Hz, 2), 7.16 (d, J = 8.6 Hz, 2), 6.89 (d, J = 8.6 Hz, 2), 5.12 (dd, J = 8.7, 3.1 Hz, 1), 4.51 (m ,1), 3.92-4.09 (2), 3.46 (dd, J = 14.2, 3.9 Hz, 1), 3.13 (dd, J = 14.2, 9.4 Hz, 1), 2.75 (brs, 1), 2.67 (q, J = 7.6 Hz, 2), 1.27 (t, J = 7.6 Hz, 3); MS (ESI+) *m/z* 394.1 (M + Na); MS (ESI-) *m/z* 370.2 (M - H).

5-[[4-[2-(4-Ethylphenyl)-2-oxoethoxy]phenyl]methyl]-2,4-thiazolidinedione 5: To a stirring solution of P_2O_5 (0.50g, 1.8 mmol) in CH_2Cl_2 (8 mL), cooled in an ice-water bath under nitrogen, was added a solution of **24a** (0.33g, 0.89 mmol) in CH_2Cl_2 (8 mL) followed by DMSO (0.32 mL, 4.4 mmol). After stirring for 15 minutes *i*-Pr_2Net (0.46 mL, 2.7 mmol) was added. The mixture was allowed to stir for 1 h, then was cast into cold (ice-water) saturated aq. $NaHCO_3$ (50 mL) and extracted with EtOAc (2 x 50 mL). The combined organic layers were washed with brine (100 mL), dried (Na_2SO_4), filtered and concentrated *in vacuo* to afford crude **5** as a sticky yellow solid. The crude product was purified by chromatography on a column of silica gel using the flash technique (20 mm OD, 30g, 230-400 mesh), eluting with 0-15% EtOAc-CH_2Cl_2. Fractions containing **5** were combined and concentrated *in vacuo* to give 236mg (72%) of **5** as a white solid. ^{1}H-NMR (400 MHz, $CDCl_3$): δ = 8.10 (brs, 1), 7.95 (d, J = 8.3 Hz, 2), 7.35 (d, J = 8.3 Hz, 2), 7.17 (d, J = 8.6 Hz, 2), 6.91 (d, J = 8.6 Hz, 2), 5.28 (s, 2), 4.51 (dd, J = 9.6, 3.9 Hz, 1), 3.48 (dd, J = 14.1, 3.9 Hz, 1), 3.12 (dd, J = 14.1, 9.6 Hz, 1), 2.75 (q, J =

7.6 Hz, 2), 1.29 (t, J = 7.6 Hz, 3); MS (ESI+) *m/z* 370.1 (M + H); MS (ESI-) *m/z* 368.1 (M - H); Anal. Calcd, for $C_{20}H_{19}NO_4S$: C, 65.02; H, 5.18; N, 3.79. Found: C, 65.13; H, 5.14; N, 3.91.

4-[2-(3-Methoxyphenyl)-2-oxoethoxy]benzaldehyde 22b: To a solution of 2-bromo-1-(3-methoxyphenyl)-ethanone 14.85g, 64.83 mmol, Aldrich) in acetone (100 mL) was added 4-hydroxybenzaldehyde (8.21g, 67.2 mmol) and potassium carbonate (9.29g, 67.2 mmol). The mixture was allowed to stir at room temperature under nitrogen for 12 hours, then the solvent was removed *in vacuo* and the residue was partitioned between CH_2Cl_2 (500 mL) and water (500 mL). The organic phase was washed with brine (500 mL), dried (Na_2SO_4) and concentrated *in vacuo* to give crude **22b** as a sticky pale yellow solid. Crude **22b** was purified by chromatography on a column of silica gel using the flash technique (50 mm OD, 150g, 230-400 mesh), eluting with CH_2Cl_2. Fractions containing the desired product were combined and concentrated *in vacuo* to afford **22b** (10.84g, 62%) as an off-white solid. ^{1}H-NMR (400 MHz, DMSO-d_6): δ = 9.88 (s, 1), 7.86 (d, J = 7.5 Hz, 2), 7.63 (m, 1), 7.51 (m, 2), 7.21 (m, 1), 7.17 (d, J = 7.5 Hz, 2), 5.76 (s, 2), 3.84 (s, 3); MS (ESI+) *m/z* 271.2 (M + H).

5-[[4-[2-(3-Methoxyphenyl)-2-oxoethoxy]phenyl]methylene]-2,4-thiazolidinedione 23b: To 4-[2-(3-methoxyphenyl)-2-oxoethoxy]benzaldehyde **22b** (5.10g, 18.9 mmol) in absolute ethanol (50 mL) was added 2,4-thiazolidinedione (2.21g, 18.8 mmol) and piperidine (0.28 mL, 2.8 mmol). The mixture was heated to reflux under nitrogen and maintained at reflux for 12 hours. The mixture was cooled to room temperature then was chilled in an ice-water bath. The resulting precipitate was collected by filtration, washed with CH_2Cl_2 and dried *in vacuo* to provide **23b** (5.48g, 76%) as a fine ivory solid. ^{1}H-NMR (400 MHz, DMSO-d_6): δ = 12.53 (brs, 1), 7.76 (s, 1), 7.63 (m, 1), 7.48-7.56 (4), 7.28 (m, 1), 7.14 (d, J = 7.5 Hz, 2), 5.70 (s, 2), 3.85 (s, 3); MS (ESI-) *m/z* 368.1 (M - H).

5-[[4-[2-(4-Methoxyphenyl)-2-hydroxyethoxy]phenyl]methyl]-2,4-thiazolidinedione 24b: To a stirring solution of $CoCl_2$-$6H_2O$ (23.5 mg, 0.077 mmol) and 2,2'-bipyridine (494mg, 3.15 mmol) in water (100 mL) and THF (100 mL) was added 1.0N aq. NaOH (10 drops) followed by $NaBH_4$ (1.98g, 52.5 mmol). The resulting deep blue mixture was cooled in an ice-water bath and a solution of **23b** (5.48g, 14.8 mmol) in THF-DMF (2:1, 75 mL) was added over 0.5 h. The reaction mixture was allowed to slowly warm to room temperature and stir

for 18 hours. Acetic acid was slowly added until the pH of the mixture was ca. 6. The mixture was diluted with water (200 mL) and extracted with CH_2Cl_2 (2 x 250 mL). The combined organic extracts were washed with brine (500 mL), dried (Na_2SO_4), filtered and concentrated *in vacuo*. The crude product was purified by chromatography on a column of silica gel using the flash technique (50 mm OD, 175g, 230-400 mesh), eluting with EtOAc-CH_2Cl_2 (1:4). Fractions containing **24b** were combined and evaporated *in vacuo* to give 4.75g (85%) of **24b** as a foamy-white solid. ^{1}H-NMR (400 MHz, $CDCl_3$): δ = 7.31 (m, 1), 7.16 (d, J = 7.4 Hz, 2), 7.00-7.05 (2), 6.82-6.91 (3), 5.12 (dd, J = 8.5, 2.9 Hz, 1), 4.51 (dd, J = 8.5, 4.6 Hz, 1), 4.51 (dd, J = 8.5, 4.6 Hz, 1), 4.18 (m, 1), 4.02 (t, J = 7.9 Hz, 1), 3.85 (s, 3), 3.45 (dd, J = 14.1, 3.9 Hz, 1), 3.12 (dd, J = 14.1, 9.3 Hz, 1), 2.75 (brs, 1); MS (ESI+) *m/z* 396.2 (M + Na); MS (ESI-) *m/z* 372.3 (M - H).

5-[[4-[2-(4-Methoxyphenyl)-2-oxoethoxy]phenyl]methyl]-2,4-thiazolidinedione 7: To a solution of 5-[[4-[2-(4-methoxyphenyl)-2-hydroxyethoxy]phenyl]methyl]-2,4-thiazolidinedione **24b** (2.82g, 7.55 mmol) in EtOAc (25 mL) was added 2-iodoxybenoic acid (1.23g, 4.4 mmol). The mixture was heated to reflux for 5 hours at which point it was judged (HPLC) to be ca. 50% complete and an additional 1.50g (5.35 mmol) of IBX was added. After an additional 5 hours at reflux, HPLC analysis indicated that the reaction was complete and the mixture was cooled to room temperature and filtered through a small pad of silica and the pad was rinsed with EtOAc. The solvent was removed *in vacuo* and the residue was purified by chromatography on a column of silica gel using the flash technique (40 mm OD, 100g, 230-400 mesh), eluting with 0-15% EtOAc-CH_2Cl_2. Fractions containing **7** were pooled to give **7** (2.15g, 77%) as a pale tan solid. ^{1}H-NMR (400 MHz, DMSO-d_6): δ = 12.03 (s, 1), 7.62 (d, J = 7.7 Hz, 1), 7.45-7.51 (2), 7.26 (m, 1), 7.16 (d, J = 8.6 Hz, 2), 6.91 (d, J = 8.6 Hz, 2), 5.55 (s, 2), 4.88 (m, 1), 3.84 (s, 3), 3.31 (dd, J = 14.2, 4.2 Hz, 1), 3.05 (dd, J = 14.2, 9.2 Hz, 1); MS (ESI+) *m/z* 394.3 (M + Na); MS (ESI-) *m/z* 370.3 (M - H); Anal. Calcd. For $C_{19}H_{17}NO_5S$ C, 61.44; H, 4.61; N, 3.77. Found: C, 61.29; H, 4.52; N, 3.57.

5-[[4-[(2*S*)-2-(5-Ethyl-2-pyridinyl)-2-hydroxyethoxy]phenyl]methyl]-2,4-thiazolidonedione 11: A stirring mixture of dichloro(η^6-*p*-cymene)ruthenium(II) dimer (15mg, 0.000025 mmol), (1*R*, 2*R*)-(-)N-p-tosyl-1,2,diphenylethylenediamine (18mg, 0.000048 mmol), and triethyl amine (30µL, 0.0002 mmol) in isopropyl alcohol (4.0 mL) was heated to reflux under nitrogen for 30 minutes. The mixture was then allowed to cool to

room temperature and was concentrated *in vacuo* to afford a dark brown solid. The dark brown solid was dissolved in DMF (5mL) and ketone **6** (0.50g, 1.30 mmol) was added in 1 portion followed by HCOOH/Et_3N (5:2, 1.00g). The mixture was allowed to stir under nitrogen for 24 hours, at which time HPLC analysis indicated that the reaction was complete. The mixture was concentrated *in vacuo* (hi-vac rotary evaporator) and the residue was partitioned between saturated aq. $NaHCO_3$ (75 mL) and CH_2Cl_2 (75 mL). The aqueous phase was extracted with CH_2Cl_2 (75 mL) and the combined organic phases were washed with water (2 x 100mL), brine (2 x 100 mL) and dried (Na_2SO_4). Concentration *in vacuo* afforded the crude alcohol **11** as a reddish foamy solid which was purified by chromatography on a column of silica gel using the flash technique (20 mm OD, 30g, 230-400 mesh), eluting with 0-10% acetone/CH_2Cl_2 followed by 10:90 acetone/CH_2Cl_2 + 0.3% MeOH. Fractions containing **11** were pooled and concentrated *in vacuo* to provide 0.410g (85%) of **11** as an off-white solid. ^{1}H-NMR (400MHz, $CDCl_3$): δ = 8.44 (d, J = 2.0 Hz, 1), 7.59 (dd, J = 8.0, 2.0 Hz, 1), 7.41 (d, J = 8.0 Hz, 1), 7.13 (d, J = 8.8 Hz, 2), 6.87 (d, J = 8.8 Hz, 2), 5.12 (t, J = 6.0 Hz, 1), 4.49 (dd, J = 9.2, 4.0 Hz, 1), 4.18 (d, J = 6.0 Hz, 2), 3.42 (dd, J = 14.4, 4.0 Hz, 1), 3.11 (dd, J = 14.0, 9.2 Hz, 1), 2.69 (q, J = 7.6 Hz, 2), 1.27 (t, J = 7.6 Hz, 3); MS (ESI+) *m/z* 373.1 (M + H), MS (ESI-) *m/z* 371.1 (M - H); $[\alpha]_D^{25}$ = -12.4° (*c* 2.0 $CHCl_3$); Anal. Calcd. For $C_{19}H_{20}N_2O_4S$: C, 61.27; H, 5.41; N, 7.52. Found: C, 61.40; H, 5.22; N, 7.76; Chiral HPLC (Chirobiotic T): 98:2, 96%ee.

5-[[4-[(2*R*)-2-(5-Ethyl-2-pyridinyl)-2-hydroxyethoxy]phenyl]methyl]-2,4-thiazolidonedione 12: A stirring mixture of dichloro(η^6-*p*-cymene)ruthenium(II) dimer (15mg, 0.000025 mmol), (1*S*, 2*S*)-(+)N-p-tosyl-1,2,diphenylethylenediamine (18mg, 0.000048 mmol), and triethyl amine (30µL, 0.0002 mmol) in isopropyl alcohol (4.0 mL) was heated to reflux under nitrogen for 30 minutes. The mixture was then allowed to cool to room temperature and was concentrated *in vacuo* to afford a dark brown solid. The dark brown solid was dissolved in DMF (5mL) and ketone **6** (0.50g, 1.30 mmol) was added in 1 portion followed by HCOOH/Et_3N (5:2, 1.00g). The mixture was allowed to stir under nitrogen for 24 hours, at which time HPLC analysis indicated that the reaction was complete. The mixture was concentrated *in vacuo* (hi-vac rotary evaporator) and the residue was partitioned between saturated aq. $NaHCO_3$ (75 mL) and CH_2Cl_2 (75 mL). The aqueous phase was extracted with CH_2Cl_2 (75 mL) and the combined organic phases were washed with water (2 x 100mL),

brine (2 x 100 mL) and dried (Na_2SO_4). Concentration *in vacuo* afforded the crude alcohol **12** as a reddish foamy solid which was purified by chromatography on a column of silica gel using the flash technique (20 mm OD, 30g, 230-400 mesh), eluting with 0-10% acetone/CH_2Cl_2 followed by 10:90 acetone/CH_2Cl_2 + 0.3% MeOH. Fractions containing **12** were pooled and concentrated *in vacuo* to provide 0.434g (90%) of **12** as an off-white solid. ^{1}H-NMR (400MHz, $CDCl_3$): δ = 8.44 (d, J = 2.0 Hz, 1), 7.59 (dd, J = 8.0, 2.0 Hz, 1), 7.41 (d, J = 8.0 Hz, 1), 7.13 (d, J = 8.8 Hz, 2), 6.87 (d, J = 8.8 Hz, 2), 5.12 (t, J = 6.0 Hz, 1), 4.49 (dd, J = 9.2, 4.0 Hz, 1), 4.18 (d, J = 6.0 Hz, 2), 3.42 (dd, J = 14.4, 4.0 Hz, 1), 3.11 (dd, J = 14.0, 9.2 Hz, 1), 2.69 (q, J = 7.6 Hz, 2), 1.27 (t, J = 7.6 Hz, 3); MS (ESI+) *m/z* 373.1 (M + H), MS (ESI-) *m/z* 371.1 (M - H); $[\alpha]_D^{25}$ = 10.8° (*c* 2.0 $CHCl_3$); Anal. Calcd. for $C_{19}H_{20}N_2O_4S$: C, 61.27; H, 5.41; N, 7.52. Found: C, 61.35; H, 5.11; N, 7.48; Chiral HPLC (Chirobiotic T): 2:98, 96%ee.

5-[[4-[(2*S*)-2-Hydroxy-2-(3-methoxyphenyl)ethoxy]phenyl]methyl]-2,4thiazolidinedione 13: A stirring mixture of dichloro(η^6-*p*-cymene)ruthenium(II) dimer (7.5mg, 0.0000125 mmol), (1*R*, 2*R*)-(-)N-p-tosyl-1,2,diphenylethylenediamine (8.9mg, 0.000025 mmol), and triethyl amine (20μL, 0.0001 mmol) in isopropyl alcohol (5.0 mL) was heated to reflux under nitrogen for 30 minutes. The mixture was then allowed to cool to room temperature and was concentrated *in vacuo* to afford a dark brown solid. The dark brown solid was dissolved in DMF (5mL) and ketone **7** (0.50g, 1.00 mmol) was added in 1 portion followed by HCOOH/Et_3N (5:2, 0.51g). The mixture was allowed to stir under nitrogen for 24 hours, at which time HPLC analysis indicated that the reaction was complete. The mixture was concentrated *in vacuo* (hi-vac rotary evaporator) and the residue was partitioned between saturated aq. $NaHCO_3$ (75 mL) and CH_2Cl_2 (75 mL). The aqueous phase was extracted with CH_2Cl_2 (75 mL) and the combined organic phases were washed with water (2 x 100mL), brine (2 x 100 mL) and dried (Na_2SO_4). Concentration *in vacuo* afforded the crude alcohol **11** as a reddish foamy solid which was purified by chromatography on a column of silica gel using the flash technique (20 mm OD, 30g, 230-400 mesh), eluting with 0-20% acetone/CH_2Cl_2. Fractions containing **13** were pooled and concentrated *in vacuo* to provide 0.50g (98%) of **13** as an off-white solid. ^{1}H-NMR (400MHz, $CDCl_3$): δ = 7.93 (brs, 1), 7.31 (t, J = 10.8 Hz, 1), 7.16 (m, 2), 7.02 (m, 2), 6.85-6.95 (3), 5.11 (dd, J = 11.6, 4.0 Hz, 1), 4.51 (dd, J = 12.4, 5.2 Hz, 1), 4.11 (dd, J = 12.4, 5.2 Hz, 1), 4.01 (m, 1), 3.84 (s, 3), 3.45 (dd, J = 18.8, 4.0 Hz, 1), 3.13 (dd,

J = 18.8, 11.6 Hz, 1); MS (ESI+) *m/z* 396.1 (M + Na), MS (ESI-) *m/z* 372.1 (M - H); $[\alpha]_D^{25}$ = 38° (*c* 11.0 $CHCl_3$); Anal. Calcd. for $C_{19}H_{19}NO_5S$: C, 61.11; H, 5.13; N, 3.75. Found: C, 61.14; H, 5.25; N, 3.66; Chiral HPLC (Chirobiotic T): 98.2, 96%ee.

5-[[4-[(2*S*)-2-Hydroxy-2-(3-methoxyphenyl)ethoxy]phenyl]methyl]-2,4thiazolidinedione 14: A stirring mixture of dichloro(η^6-*p*-cymene)ruthenium(II) dimer (8.1mg, 0.000090 mmol), (1*S*, 2*S*)-(+)N-p-tosyl-1,2,diphenylethylenediamine (9.6mg, 0.000026 mmol), and triethyl amine (20μL, 0.0001 mmol) in isopropyl alcohol (5.0 mL) was heated to reflux under nitrogen for 30 minutes. The mixture was then allowed to cool to room temperature and was concentrated *in vacuo* to afford a dark brown solid. The dark brown solid was dissolved in DMF (5mL) and ketone **7** (0.55g, 1.5 mmol) was added in 1 portion followed by $HCOOH/Et_3N$ (5:2, 0.55g). The mixture was allowed to stir under nitrogen for 24 hours, at which time HPLC analysis indicated that the reaction was complete. The mixture was concentrated *in vacuo* (hi-vac rotary evaporator) and the residue was partitioned between saturated aq. $NaHCO_3$ (75 mL) and CH_2Cl_2 (75 mL). The aqueous phase was extracted with CH_2Cl_2 (75 mL) and the combined organic phases were washed with water (2 x 100mL), brine (2 x 100 mL) and dried (Na_2SO_4). Concentration *in vacuo* afforded the crude alcohol **11** as a reddish foamy solid which was purified by chromatography on a column of silica gel using the flash technique (20 mm OD, 30g, 230-400 mesh), eluting with 0-20% acetone/CH_2Cl_2. Fractions containing **13** were pooled and concentrated *in vacuo* to provide 0.53g (96%) of **14** as an off-white solid. ^{1}H-NMR (400MHz, $CDCl_3$): δ = 7.93 (brs, 1), 7.31 (t, J = 10.8 Hz, 1), 7.16 (m, 2), 7.02 (m, 2), 6.85-6.95 (3), 5.11 (dd, J = 11.6, 4.0 Hz, 1), 4.51 (dd, J = 12.4, 5.2 Hz, 1), 4.11 (dd, J = 12.4, 5.2 Hz, 1), 4.01 (m, 1), 3.84 (s, 3), 3.45 (dd, J = 18.8, 4.0 Hz, 1), 3.13 (dd, J = 18.8, 11.6 Hz, 1); MS (ESI+) *m/z* 396.1 (M + Na), MS (ESI-) *m/z* 372.1 (M - H); $[\alpha]_D^{25}$ = -34° (*c* 11.0 $CHCl_3$); Anal. Calcd. for $C_{19}H_{19}NO_5S$: C, 61.11; H, 5.13; N, 3.75. Found: C, 61.23; H, 5.29; N, 3.71; Chiral HPLC (Chirobiotic T): 2:98, 96%ee.

References

1. Scoccio, R.E.; Chen, E.R.; Lazar, M.A. Thiazolidinediones and the promise of insulin sensitization in type 2 diabetes *Cell Metab.* **2014**, *20*, 573-91 https://DOI:10.1016/j.cmet.2014.08.005

2. Colca, J.R.; Kletzien, R.F. What has prevented the expansion of insulin sensitizers? *Expert Opin. Investig. Drugs* **2006**, *15*, 205-210 https://doi.org/10.1517/13543784.15.3.205

3. Colca, J.R.; Tanis, S.P.; McDonald, W.G.; Kletzien, R.F. Insulin sensitizers in 2013: new insights for the development of novel therapeutics agents to treat metabolic diseases *Expert Opin. Investig. Drugs* **2014**, *23,* 1-7 https://doi.org/10.1517/13543784.2013.839659

4. Colca, J.R. The TZD insulin sensitizer clue provides a new route into diabetes drug discovery *Expert Opin. Drug Discov.* **2015**, *10*, 1259-1270 https://doi.org/10.1517/17460441.2015.1100164

5. Sohda, T.; Meguro, K.; Kawamatsu, Y. Studies on antidiabetic agents. IV. Synthesis and activity of the metabolites of 5-[4-(1-methylcyclohexylmethoxy)benzyl]-2,4-thiazolidinedione (ciglitazone) *Chem. Pharm. Bull.* **1984**, *32*, 2267-78 https://doi.org/10.1248/cpb.32.2267

6. Hofmann, C.A.; Colca, J.R. New oral thiazolidinedione antidiabetic agents act as insulin sensitizers *Diabetes Care* **1992**, *15*, 1075-8 https://doi.org/10.2337/diacare.15.8.1075

7. Yki-Jaervinen, H. Thiazolidinediones *N. Engl. J. Med.* **2004**, *351*, 1106-18

8. Lehmann, J.M.; Moore, L.B.; Smith-Oliver, T.A.; Wilkison, W.O.; Willson, T.M.; Kliewer, S.A. An antidiabetic thiazolidinedione is a high affinity ligand for peroxisome proliferator-activated receptor γ (PPARγ) *J. Biol. Chem.* **1995**, *270*, 12953-6 https://doi.org/10.1074/jbc.270.22.12953

9. Olefsky, J.M.; Saltiel, A.R. PPARγ and the treatment of insulin resistance *Trends in Endocrinol. Metab.* **2000**, *11*, 362-8 https://doi.org/10.1016/S1043-2760(00)00306-4

10. Peraza, M.A.; Burdick, A.D.; Marin, H.E.; Gonzalez, F.J.; Peters, J.M. The toxicology of ligands for peroxisome proliferator-activated receptors (PPAR) *Toxicol. Sci.* **2006**, *90*, 269-95 https://doi.org/10.1093/toxsci/kfj062

11. Bloomgarden, Z.T. Treatment issues in type-2 diabetes *Diabetes Care* **2002**, *25*, 390-4 https://doi.org/10.2337/diacare.25.2.390

12. Rucker, C.; Scaarsi, M.; Meringer, M. 2D QSAR of PPARγ agonist binding and transactivation *Bioorg. Med. Chem.* **2006**, *14*, 5178-95 https://doi.org/10.1016/j.bmc.2006.04.005

13. Kletzien, R.F.; Clarke, S.D.; Ulrich, R,G. Enhancement of adipocyte differentiation by an insulin

sensitizing agent *Mol. Pharmacol.* **1992**; *41*, 393-8
http://molpharm.aspetjournals.org/content/41/2/393

14. Martin, J.A.; Brooks, D.A.; Prieto, L.; Gonzalez, R.; Torrado, A.; Rojo, I.; Lopez de Uralde, B.; Lamas, C.; Ferritto, R.; Dolores Martin-Ortega, M.; Agejas, J.; Parra, F.; Rizzo, J.R.; Rhodes, G.A.; Robey, R.L.; Alt, C.A.; Wendel, S.R.; Zhang, T.Y.; Reifel-Miller, A.; Montrose-Rafizadeh, C.; Brozinick, J.T.; Hawkins, E.; Misener, E.A.; Briere, D.A.; Ardecky, R.; Fraser, J.D.; Warshawsky, A.M. 2-Alkoxydihydrocinnamates as PPAR agonists. Activity modulation by the incorporation of phenoxy substituents *Bioorg. Med. Chem. Lett.* **2005**, *15*, 51-5
https://doi.org/10.1016/j.bmcl.2004.10.042
15. Haigh, D..; Allen, G.; Birrell, H.C.; Buckle, D.R.; Cantello, B.C.C.; Eggleston, D.S.; Haltiwanger, R.C.; Holder, J.C.; Lister, C.A.; Pinto, I.L.; Rami, H.K.; Sime, J.T.; Smith, S.A.; Sweeney, J.D. Non-thiazolidinedione antihyperglycemic agents. Part 3: The effects of stereochemistry on the potency of α-methoxy-β-phenylpropanoic acids *Bioorg. Med. Chem.* **1999**, *7*, 821-30
https://doi.org/10.1016/S0968-0896(99)00034-6
16. Azukizawa, S.; Kasai, M.; Takahashi, K.; Miike, T.; Kunishiro, K.; Kanda, M.; Mukai, C.; Shirahase, H. Synthesis and biological evaluation of (S)-1,2,3,4-tetrahydroisoquinoline-3-carboxylic acids: a novel series of PPARγ agonists *Chem. Pharm. Bull*. **2008**, *56*, 335-45
https://doi.org/10.1248/cpb.56.335
17. Liu, K.G.; Lambert, M.H.; Ayscue, A.H.; Henke, B.R.; Leesnitzer, L.M.; Oliver, W.R., Jr.; Plunket, K.D.; Xu, H.E.; Sternbach, D.D.; Willson, T.M. Synthesis and biological activity of L-tyrosine-based PPARγ agonists with reduced molecular weight *Bioorg. Med. Chem. Lett*. **2001**, *11*, 3111-13
https://doi.org/10.1016/S0960-894X(01)00649-7
18. Lu, Y.; Guo, Z.; Guo, Y.; Feng, J.; Chu, F. Design, synthesis and evaluation of 2-alkoxydihydrocinnamates as PPAR agonists *Bioorg. Med. Chem. Lett*. **2006**, *16*, 915-919
https://doi.org/10.1016/j.bmcl.2005.10.104
19. Pirat, C.; Farce, A.; Lebegue, N.; Renault, N.; Furman, C.; Millet, R.; Yous, S.; Speca, S.; Berthelot,

P.; Desreumaux, P.; Chavatte, P. Targeting peroxisome proliferator-activated receptors (PPARs): development of modulators *J. Med. Chem*. **2012**, *55*, 4027-61 https://pubs.acs.org/doi/full/10.1021/jm101360s

20. Kliewer, S.A.; Xu, H.E.; Lambert, M.H.; Willson, T.M. Peroxisome proliferator-activated receptors: from genes to physiology *Recent Prog. Horm. Res.* **2001**, *56*, 239-263 https://doi.org/10.1210/rp.56.1.239

21. (a) Colca, J.R. Insulin sensitizers may prevent metabolic inflammation *Biochem. Pharmacol.* **2006**, *72*, 125-131 https://doi.org/10.1016/j.bcp.2006.01.002; (b) Burant, C.F.; Sreenan, S.; Hirano, K.; Tai, T.A.; Lohmiller, J.; Lukens, J.; Davodspm, N.O.; Ross, S.; Graves, R.A. Troglitazone action is independent of adipose tissue *J. Clin. Invest.* **1997**, *100*, 2900-2908 https://doi.org/10.1172/JCI119839

22. Chen, Z.; Vigueira, P.A.; Chambers, K.T.; Hall, A.M.; Mitra, M.S.; Qi, N.; McDonald, W.G.; Colca, J.R.; Kletzien, R.F.; Finck, B.N. Insulin resistance and metabolic derangement in obese mice are ameliorated by a novel peroxisome proliferator-activated receptor γ-sparing thiazolidinedione *J. Biol Chem.* **2012**, *287*, 23537-23548 http://www.jbc.org/content/287/28/23537

23. Winkelmayer, W.C.; Setoguchi, S.; Levin, R.; Solomon, D.K. Comparison of cardiovascular outcomes in elderly patients with diabetes who initiated rosiglitazone vs pioglitazone therapy *Arch. Intern. Med.* **2008**, *168*, 2368-75 https://doi.org/10.1001/archinte.168.21.2368

24. Ryder. R.E.J. Pioglitazone: an agent which reduces stroke, myocardial infarction and death and is also a key component of the modern paradigm for the optimum management of type-2 diabetes *Br. J. Diabetes Vasc. Dis.* **2011**, *11*, 113-20 https://doi.org/10.1177/1474651411412658

25. Henry, R.R.; Erikson, D.; Ciraldi, T.A. PPARγ agonists and the future for insulin sensitizers *Br. J. Diabetes Vasc. Dis.* **2012**, *12*, 206-10 https://doi.org/10.1177/1474651412459202

26. (a) Heneka, M.T.; Fink, A.; Doblhammer, G. Effect of pioglitazone medication on the incidence of dementia *Ann. Neurol.* **2015**, *78*, 284-294 https://doi.org/10.1002/ana.24439; (b) Young, L.H.; Viscoli, C.M.; Curtis, J.P.; Inzucchi, S.E.; Schwartz, G.G.; Lovejoy, A.M.; Furie, K.L.; Gorman,

M.J.; Conwit, R.; Abbot, J.D.; Jacoby, D.L.; Kolansky, D.M.; Pfau, S.E.; Ling, F.S.; Kernan, W.N. Cardiac outcomes after ischemic stroke or transient ischemic attack: effects of pioglitazone in patients with insulin resistance without diabetes mellitus *Circulation,* **2017**, 135, 1882-1893 https://www.ahajournals.org/doi/10.1161/CIRCULATIONAHA.116.024863; (c) Yaghi, S.; Furie, K.L.; Viscoli, C.M.; Kamel, H.; Gorman, M.; Dearborn, J.; Young, L.H.; Inzucchi, S.E.; Lovejoy, A.M.; Kasner, S.E.; Conwit, R. Kernan, W.N. Pioglitazone prevents stroke in patients with a recent transient ischemic attack or ischemic stroke: a planned secondary analysis of the IRIS trial (insulin resistance intervention after stroke) *Circulation*, **2018**, *137*, 455-463 https://www.ahajournals.org/doi/10.1161/CIRCULATIONAHA.117.030458

27. Feinstein, D.L.; Spagnolo, A.; Akar, C.; Weinberg, G.; Murphy, P.; Gavrilyuk, V.; Russo, C.D. Receptor-independent actions of PPAR thiazolidinedione agonists: is mitochondrial function the key? *Biochem. Pharmacol.* **2005**, *70*, 177-188 https://doi.org/10.1016/j.bcp.2005.03.033

28. (a) Colca, J.R.; McDonald, W.G.; Waldon, D.J.; Leone, J.W.; Lull, J.M.; Bannow, C.A.; Lund, E.T.; Mathews, W.R. Identification of a novel mitochondrial protein ("mitoNEET") cross-linked specifically by a thiazolidinedione photoprobe *Am. J. Physiol.* **2004**, *286* (2, pt. 1), 252-260 https://doi.org/10.1152/ajpendo.00424.2003; (b) Colca, J.R.; McDonald, W.G.; Cavey, G.S.; Cole, S.L.; Holewa, D.D.; Brightwell-Conrad, A.S.; Wolfe, C.L.; Wheeler, J.S.; Coulter, K.R.; Kilkuskie, P.M.; Gracheva, E.; Korshunova, Y.; Trusgnich, M.; Karr, R.; Wiley, S.E.; Divakaruni, A.S.; Murphy, A.N.; Vigueira, P.A.; Finck, B.N.; Kletzien, R.F. Identification of a mitochondrial target of thiazolidinedione insulin sensitizers (mTOT) – relationship to newly identified mitochondrial pyruvate carrier proteins *PLoS One* **2013**, *8*, e61551 https://doi.org/10.1371/journal.pone.0061551; (c) Colca, J.R.; McDonald, W.G.; Kletzein, R.F. Mitochondrial target of thiazolidinediones *Diabetes, Obes. Metab.* **2014**, *16*, 1048-1054 https://doi.org/10.1111/dom.12308

29. (a) Colca, J.R.; McDonald, W.G.; McCommis, K.S.; Finck, B.M. Treating fatty liver disease by modulating mitochondrial pyruvate metabolism *Hepatology Commun.* **2017**, *1*, 193-197 https://doi.org/10.1002/hep4.1036; (b) Bricker, D.K.; Taylor, E.B.; Schell, J.C.; Orsak. T.; Boutron,

A.; Chen, Y-C.; Cox, J.E.; Cardon, C.M.; Van Vranken, J.G.; Dephoure, N.; Redin, C.; Boudina, S.; Gygi, S.P.; Brivet, M.; Thummel, C.S.; Rutter, J. A mitochondrial pyruvate carrier required for pyruvate uptake in yeast, drosphilia, and humans *Science* **2012**, *337*, 96-100 https://doi.org/10.1126.science.1218099; (c) Herzig. S.; Raemy, E.; Montessuit, S.; Veuthey, J.L.; Zamboni, N.; Westermann B.; Kunji, E.R.S.; Martinou, J-C. *Science* **2012**, *337*, 93-96 https://doi.org/10.1126/science.1218530

30. (a) Colca J.R.; VanderLugt, J.T.; Adams, W.J.; Shashlo, A.; McDonald, W.G.; Liang J.; Zhou, R.; Orloff, D.G. Clinical proof-of-concept study with MSDC-0160, a prototype mTOT-modulating insulin sensitizer *Clin. Pharmacol. Ther.* **2013**, *93*, 352-359 https://doi.org/10.1038/clpt.2013.10; (b) McCommis, K.S.; Chen, Z.; Fu, X.; McDonald, W.G.; Colca, J.R.; Kletzien, R.F.; Burgess, S.C.; Finck, B.N. Loss of mitochondrial pyruvate carrier 2 in the liver leads to defects in gluconeogenesis and compensation via pyruvate-alanine cycling *Cell Metab.* **2015**, *22*, 682-694 https://doi.org/10.1016/j.cmet.2015.07.028
31. (a) Ghosh, A.; Tyson, T.; George, S.; Hildebrandt, E.N.; Steiner, J.A.; Schulz, E.; Machiela, E.; Escobar, G.M.L.; Kordower, J.H.; Van Raamsdonk, J.M; Brundin, P.; Madaj, Z.; McDonald, W.G.; Colca, J.R.; Kordower, J.H. Mitochondrial pyruvate carrier regulates autophagy, inflammation, and neorudegeneration in experimental models of parkinson's disease *Sci. Transl. Med.* **2016**, *8*, 368ra174/1-368ral174/18 https://doi.org/10.1126/scitranslmed.aag2210; (b) Shah, R.C.; Matthews, D.C.; Andrews, R.D.; Capuano, A.W.; Fleischman, D.A.; VanderLugt, J.T.; Colca, J.R. An evaluation of MSDC-0160, a prototype mTOT modulating insulin sensitizer, in patients with mild alzheimer's disease *Curr. Alzheimer Res.* **2014**, *11*, 564-573 https://doi.org/10.2174/1567205011666140616113406
32. McCommis, K.S.; Hodges, W.T.; Brunt, E.M.; Nalbantoglu, I.; McDonald, W.G.; Holley, C.; Fujiwara, H.; Schaffer, J.E.; Colca, J.R.; Finck, B.N. Targeting the mitochondrial pyruvate carrier attenuates fibrosis in a mouse model of nonalcoholic steatohepatitis *Hepatology* **2017**, *65*, 1543-1556 https://doi.org/10.1002/hep.29025

33. (a) Yang, C.; Ko, B.; Hensley, C.T.; Jiang, L.; Wasti, A.T.; Kim, J.; Sudderth, J.; Calvaruso, M.A.; Lumata, L.; Mitsche, M.; Rutter, J.; Merritt, M.E.; DeBerardinis, R.J. Glutamine oxidation maintains the TCA cycle and cell survival during impaired mitochondrial pyruvate transport *Mol. Cell* **2014**, *56*, 414-424 https://doi.org/10.1016/j.molcel.2014.09.025; (b) Vacanti, N.M.; Divakaruni, A.S.; Green, C.R.; Parker, S.J.; Henry, R.R.; Ciaraldi, T.P.; Murphy, A.N.; Metallo, C.M. Regulation of substrate utilization by the mitochondrial pyruvate carrier *Mol. Cell* **2014**, *56*, 425-435 https://doi.org/10.1016/j.molcel.2014.09.024; (c) Perry, R.J.; Camporez, J-P.G.; Kursawe, R.; Titchenell, P.M.; Zhang, D.; Perry, C. J.; Jurczak, M.J.; Abudukadier, A.; Han, M.S.; Zhang, X-M.; Ruan, H-B.; Yang, X.; Caprio, S.; Kaech, S.M.; Sul, H.S.; Birnbaum, M.J.; Davis, R.J.; Cline, G.W.; Petersen, K.F.; Shulman, G.I. Hepatic acetyl CoA links adipose tissue inflammation to hepatic insulin resistance and type 2 diabetes *Cell* **2015**, *160*, 745-758 https://doi.org/10.1016/j.cell.2015.01.012

34. (a) Ochocki, J.D.; Simon, M.C. Nutrient-sensing pathways and metabolic regulation in stem cells *J. Cell. Biol.* **2013**, *203*, 23-33; (b) Shyh-Chang, N.; Daley, G.Q.; Cantley, L.C. Stem cell metabolism in tissue development and aging *Development* **2013**, *140*, 2535-2547 https://doi.org/10.1242/dev.091777

35. (a) LeBrasseur, N.K.; Kelly, M.; Tsao, T-S.; Farmer, S.R.; Saha, A.K.; Ruderman, N.B.; Tomas, E. Thiazolidinediones can rapidly activate AMP-activated protein kinase in mammalian tissues *Am. J. Physiol. Endocrinol. Metab.* **2006**, *291*, E175-81 https://doi.org/10.1152/ajpendo.00453.2005; (b) He, G.; Sung, Y.M.; DiGiovanni, J.; Fischer, S.M. Thiazolidinediones inhibit insulin-like growth factor-1-induced activation of p70s6 kinase and suppress insulin-like growth factor-1 tumor promoting activity *Cancer Research* 2006, 66, 1873-1878 https://doi.org/10.1158/0008-5472.CAN-05-3111 (c) Han, S.W.; Zheng, Y.; Roman, J. Rosiglitazone, an agonist of PPARγ, inhibits non-small cell carcinoma cell proliferation in part through activation of tumor sclerosis complex-2 *PPAR Res.* **2007**, *2007*, Article ID 29632 https://dx.doi.org/10.1155/2007/29632

36. Devasthale, P.V.; Chen, S.; Jeon, Y.; Qu, F.; Shao, C.; Wang, W.; Zhang, H.; Farrelly, D.; Golla, R.; Grover, G.; Harrity, T.; Ma, Z.; Moore, L.; Ren, J.; Seethala, R.; Cheng, L.; Sleph, P.; Sun, W.; Tieman, A.; Wetterau, J.R.; Doweyko, A.; Chandrasena, G.; Chang, S.Y.; Humphreys, W.G.;

Sasseville, V.G.; Biller, S.A.; Ryono, D.E.; Selan, F.; Hariharan, N.; Cheng, P.T.W. Design and synthesis of N-[(4-methoxyphenoxy)carbonyl]-N-[[4-[2-(5-methyl-2-phenyl-4-oxazolyl)ethoxy]phenyl]methyl]glycine [muraglitazar/BMS-298585], a novel peroxisome proliferator-activated receptor α/γ dual agonist with efficacious glucose and lipid lowering activities *J. Med. Chem.* **2005**, *48*, 2248-2250 https://doi.org/10.1021/jm0496436

37. Calculated using ACD Labs Structure Designer V12.0.
38. Tanis, S.P.; Parker, T.T.; Colca, J.R.; Fisher, R.M.; Kletzein, R.F. Synthesis and biological activity of metabolites of the antidiabetic, antihyperglycemic agent pioglitazone *J. Med. Chem.* **1996**, *39*, 5053-5063 https://doi.org/10.1021/jm9605694
39. Taber, D.F.; Amedio, J.C., Jr.; Jung, K-Y. Phosphorus pentoxide/dimethyl sulfoxide/trimethylamine (PDT): a convenient procedure for oxidation of alcohols to ketones and aldehydes *J. Org. Chem.* **1987**, *52*, 5621-5622 https://doi.org/10.1021/jo00234a021
40. Colca, G.R.; Larsen, S.D.; Tanis, S.P.; Parker, T.; Gadwood, R. Thiazolidinedione analogs **WO2010105048**.
41. Carpenter, D.E.; Imbordino, R.J.; Maloney, M.T.; Moselein, J.A.; Reeder, M.R.; Scott, A. Process development and scale-up of the potential thiazolidinedione antidiabetic candidate PNU-91325 *Org. Proc. Res. Dev.* **2002**, *6*, 721-728 https://doi.org/10.1021/op025549s
42. (a) Human PPARγ Competitive Binding: The commercially available TR-FRET competitive binding assay (Invitrogen #PV4894) was used to measure binding affinity for PPARγ. (b) Human PPARγ Transactivation – Agonist Assay: A commercially available gene reported assay from Invitrogen (Catalog #K1419) was used to measure the transactivation of PPARγ.
43. (a) Sohda, T.; Momose, Y.; Meguro, K.; Kawamatsu, Y.; Sugiyama, Y.; Ikeda, H. Studies on antidiabetic agents. Synthesis and hypoglycemic activity of 5-[4-(pyridylalkoxy)benzyl]-2,4-thiazolidinediones *Arzneim-Forsch.* **1990**, *40*, 37-42; (b) Hofmann, C.; Lorenz, K.; Colca, J. R. Glucose transport deficiency in diabetic animals is corrected by treatment with the oral antihyperglycemic agent pioglitazone *Endocrinology* **1991**, *129*, 1915-1925 https://doi.org/endo-129-

4-1915; (c) Sohda, T.; Mizuno, K.; Kawamatsu, Y. Studies on antidiabetic agents. VI. Asymmetric transformation of (+/-)-5-[4-(1-methylcyclohexylmethoxy)benzyl]-2,4-thiazolidinedione (ciglitazone) with optically active 1-phenylethylamines *Chem. Pharm. Bull.* **1984**, *32*, 4460-4465 https://doi.org/10.1248/cpb.32.4460; (d) The KKAy mouse assay was carried out as previously described[2] at PharmOptima (Kalamazoo, MI).

44. (a) Tanis, S.P.; Evans, B.R.; Nieman, J.A.; Parker, T.T.; Taylow, W.D.; Heasley, S.E.; Herrinton, P.M.; Perrault, W.R.; Hohler, R.A.; Dolak, L.A.; Hester, M.A.; Seest, E.P. Solvent and in situ catalyst preparation impacts upon Noyori reductions of aryl chloromethyl ketones: application to the syntheses of chiral 2-amino-1-arylethanols *Tetrahedron Asymmetry* **2006**, *17*, 2154-2182 https://doi.org/10.1016/j.tetasy.2006.07.017

45. Divakaruni, A.S.; Wiley, S.E.; Rogers, G.W.; Andreyev, A.Y.; Petrosyan, S.; Loviscach, M.; Wall, E.A.; Yadava, N.; Heuck, A.P.; Ferrick, D.A.; Henry, R.R.; McDonald, W.G.; Colca, J.R.; Simon, M.I.; Ciaraldi, T.P.; Murphy, A.N. Thiazolidinediones are acute, specific inhibitors of the mitochondrial pyruvate carrier *Proc. Natl. Acad. Sci. USA*, **2013**, *110*, 5422-5427 https://doi.org/10.1073/pnas.1303360110

46. (a) *Molecular Operating Environment (MOE)*, 2018.01; Chemical Computing Group ULC, 1010 Sherbrooke St. West, Suite #910, Montreal, QC, Canada, H3A 2R7, 2018.

47. Lee, M.A.; Tan, L.; Yang, H.; Im, Y.-G. Structures of PPARγ complexed with lobeglitazone and pioglitazone reveal key determinants for the recognition of antidiabetic drugs *Sci. Rep.* **2017**, *7*, 16837-16837 https://www.nature.com/articles/s41598-017-17082-x

48. (a) Liberato, M.V., Nascimento, A.S., Ayers, S.D., Lin, J.Z., Cvoro, A., Silveira, R.L., Martinez, L., Souza, P.C., Saidemberg, D., Deng, T., Amato, A.A., Togashi, M., Hsueh, W.A., Phillips, K., Palma, M.S., Neves, F.A., Skaf, M.S., Webb, P., Polikarpov, I. Medium chain fatty acids are selective peroxisome proliferator activated receptor (PPAR) γ activators and pan-PPAR partial agonists *Plos One* **2012**, 7, e36297-e36297 https://doi.org/10.1371/journal.pone.0036297 ; (b) Rajapaksha, H.; Bhatia, H.; Wegener, K.; Petrovsky, N.; Bruning, J.B. X-ray crystal structure of

rivoglitazone bound to PPARγ and PPAR subtype selectivity of TZDs *Biochim. Biophys. Acta* **2017**, *1861*, 1981-199 https://doi.org/10.1016/j.bbagen.2017.05.008 .

49. Fukunaga, T.; Zoul, W.; Rohatgi, N.; Colca, J.R.; Tietlbaum, S.L. An insulin-sensitizing thiazolidinedione, which minimally activates PPARγ, does not cause bone loss *J. Bone Mineral Res.* **2015**, *30*, 481-488 https://doi.org/10.1002/jmbr.2364
50. Adams, W.J.; Dotzauer, H.M.; VanNoord, T.; Colca, J.R. *17th North American Regional ISSX Meeting* 16-20 October 2011, Abstract – p307 http://issx.confex.com/issx/17NA/webprogram/Paper25305.html
51. Colca, J.R.; McDonald, W.G.; Adams, W.J. MSDC-0602K, a metabolic modulator directed at the core pathology of NASH *Expert Opin. Investig. Drugs* **2018**, *27*, 631-636 https://doi.org/10.1080/13543784.2018.1494153
52. Still, W. C.; Kahn, M.; Mitra, A. Rapid chromatographic technique for preparative separations with moderate resolution *J. Org. Chem.* **1978**, *43*, 2923-2925 https://doi.org/10.1021/jo00408a041